CJC Chinese Journal of Chemistry 中国化学 · An International Journal

Review

Cite this paper: *Chin. J. Chem.* **2024**, *42*, XXX—XXX. **DOI: 10.1002/cjoc.202400XXX**

Biomimetic and biological applications of DNA coacervates

Yuqi Zeng,[‡,a] Long Zhao,[‡,a] Yihao Liu,[a] Tianhuan Peng, *[,a] Yifan Lyu, *[,a,b] and Quan Yuan*[,a]

[a] *Molecular Science and Biomedicine Laboratory (MBL), State Key Laboratory of Chemo/Biosensing and Chemometrics, College of Biology, College of Chemistry and Chemical Engineering, Aptamer Engineering Center of Hunan Province, Hunan University, Changsha 410082, China*
[b] *Furong Laboratory, Changsha 410082, China*

Keywords

DNA coacervates | liquid-liquid phase separation (LLPS) | cell mimicking | biosensing | nucleic acids | self-assembly

Comprehensive Summary

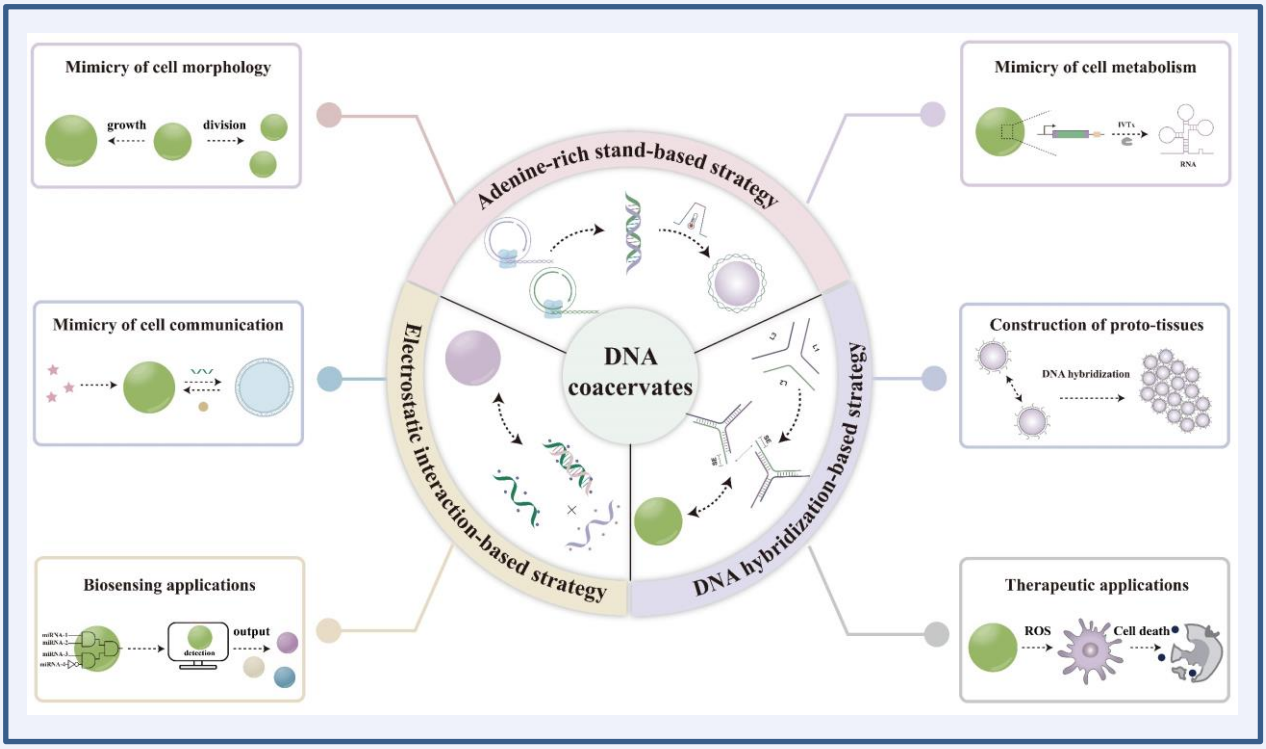

Recent progress in nanotechnology and synthetic biology has demonstrated the potential of DNA coacervates for biomimetic and biological applications. DNA coacervates are micron-scale, membrane-free, spherical structures formed by liquid-liquid phase separation of DNA materials. They uniquely combine the programmability of DNA with the fluidic properties of coacervates, allowing for controlled modulation of their structures, biomimetic and biological functions, and dynamic behaviors through rational sequence design. This review summarizes methods for the formation of different DNA coacervates and explores their extensive applications in biomimicry, biosensing and therapeutics. Limitations and prospects of DNA coacervates are also discussed.

Key Scientists

‡These authors contributed equally.
*E-mail: pengtianhuan@hnu.edu.cn, lvyifan1990@hnu.edu.cn, yuanquan@whu.edu.cn

Below is a list of scientists who have made significant contributions to the synthesis and application of DNA coacervates.

Alexander Oparin

The Department of Plant Biochemistry, Lomonosov Moscow State University

1924

Proposed that life might have originated in condensed liquid droplets

1929

Bungenberg de Jong

The Department of Physical Chemistry, Leiden University

First construction of coacervates using polycationic and polyanionic

Gary Felsenfeld

Laboratory of Molecular Biology, California Institute of Technology (Caltech)

1969

First construction of DNA coacervates by electrostatic interactions

J. Thomas August

The Department of Pharmacology and Molecular Sciences, School of Medicine, Johns Hopkins University

1995

DNA coacervates as a gene delivery vehicle

Tommaso Bellini

The Department of Medical Biotechnology and Translational Medicine, Università degli Studi di Milano

2013

First discuss the LLPS behavior of DNA motifs

Andreas Walther

Macromolecular Materials and Systems at the Department of Chemistry, Johannes Gutenberg University in Mainz

2018

The first formation of DNA coacervates by LLPS of A-rich long ssDNA

Masahiro Takinoue

The Department of Computer Science, Institute of Science Tokyo

2020

Using DNA coacervates for logical computation

Lorenzo Di Michele

The Department of Chemical Engineering and Biotechnology, University of Cambridge

2021

Achieving spatial control over the functionality of DNA Coacervates

Stories to be Continued ...

Contents

1. Introduction

Cells contain a variety of intracellular "droplets" or membraneless organelles that play crucial roles in diverse biochemical processes.[1] Examples include nucleoli within the nucleus,[2] Cajal bodies,[3] as well as stress granules and P granules found in the cytoplasm.[4] These intracellular "droplets" or membraneless organelles, also known as biomolecular coacervates,[1] are compartmentalized structures formed within cells through liquid-liquid phase separation (LLPS) of proteins, nucleic acids, lipids, and small molecules. In 1924, Alexander Oparin proposed the hypothesis that coacervates might act as scaffolds of prebiotic chemistry in early Earth and facilitate the emergence of life because the liquid-like fluidity, dynamic assembly, and disassembly capabilities, crowded internal environments of coacervates could recruit biological molecules and promote early metabolic reactions.[5] Since then, numerous efforts have been performed to investigate the possible molecular mechanisms in a protocell by mimicking metabolic processes using "bottom-up" constructed coacervates.[6]

Since the formation of coacervates is driven by electrostatic interactions, hydrophobic effects, π-stacking, and hydrogen bonding, the commonly used materials for preparing coacervates are mainly oligomers or polymer molecules rich in charges and hydrogen bonds, e.g., nucleic acid, proteins, polysaccharides, and other cationic/anionic polymers. Among these materials, DNA exhibits obvious merits, including high programmability, easy chemical modification, low immunogenicity, and superior biocompatibility.[7] Therefore, combining the unique properties of DNA and LLPS, DNA coacervates formed primarily or exclusively by DNA have been widely employed in the field of biomimicry, biosensing, and biomedicine.[8]

In this review, we focus on the preparation pathways of DNA coacervates and explore their biomimetic and biological applications. First, we describe the mechanisms behind the formation of different kinds of DNA coacervates. Subsequently, we explore the potential of DNA coacervates as synthetic cells, with a particular focus on their use in mimicking cellular behaviors, cell communication, and tissue formation. The potential applications of DNA coacervates in biosensing and biomedicine are also summarized. Finally, we discuss the challenges and prospects for the advancement of DNA coacervates in biomimetic and biological applications. It should be noted that coacervates are also referred to as "condensates" or "droplets" in other literature. In this review, we use coacervates because it is a more widely recognized name.

2. Synthesis Pathways of DNA Coacervates

Several methods for synthesizing DNA coacervates have been reported. All these DNA coacervates exhibit a liquid chamber structure in which DNA is enriched, maintaining an internal chemical composition distinct from that of the external environment. The formation of such heterogeneous systems will inevitably be influenced by some factors. Therefore, in this section, we categorize synthesis pathways of DNA coacervates, including the electrostatic interaction-based strategy, DNA hybridization-based strategy, and adenine-rich (A-rich) strand-based strategy and discuss the factors influencing the formation of DNA coacervates in each strategy.

2.1. Electrostatic interaction-based strategy

The increase in entropy caused by electrostatic interactions between oppositely charged molecules can promote molecular aggregation and the rearrangement of bound water, therefore driving LLPS. Specifically, whether coacervates or solid precipitates form depends on factors such as length, charge density, and type of macromolecules involved.[9] In this process, coacervates refer to the spontaneous formation of a polymer-rich liquid phase and a polymer-poor phase in dynamic equilibrium, driven by electrostatic interactions of molecules with opposite charges in an aqueous solution.[10] Bungenberg et al. first described this process in a mixture composed of gelatin (polycationic) and gum arabic (polyanionic).[11] Since nucleic acids are negatively charged under physiological conditions[12] due to the phosphate groups in the backbone, nucleic acids can easily interact with positively charged substances to form coacervates through LLPS. For example, the formation of some small intracellular droplets or membraneless organelles is primarily due to weak interactions between negatively charged RNA and positively charged proteins.[13,14]

Inspired by the formation of membraneless organelles in cells, researchers have begun to explore the use of negatively charged DNA in combination with cationic polymers (such as DEAE-dextran and polydiallyl dimethyl ammonium chloride (PDDA)),[15-18] cationic proteins,[19-21] and cationic peptides (such as polylysine (PLL)[22-25]) to induce LLPS and construct DNA coacervates. Shapiro et al. generated highly hydrated spherical DNA coacervates through the phase separation of long-stranded DNA and PLL.[26] Subsequently, Vieregg et al. investigated mixtures of DNA with various polycations, including PLL and short polyamines, and explored how the properties of these polymers and the salt ion concentration affect the formation of DNA coacervates.[27] Liu et al. prepared coacervates by using single-stranded DNA (ssDNA) with a G-quadruplex conformation to interact with the binding protein SERBP1 and found the aggregation and depolymerization of coacervates could be regulated by temperature (Figure 1a).[19] Yin et al. controlled the initiation, duration, and termination of complex kinetic behaviors of coacervates, such as transient compartmentalization, growth fusion, and molecular trapping, by confining condensed microdroplets of PLLs and short ssDNA within a microfluidic channel and applying a series of electric field strengths.[25] Wee et al. developed light-controlled coacervates using ssDNA, PLL, and arylazopyrazole (AAP), which can be depolymerized under ultraviolet (UV) irradiation and reassembled under green light.[28] The photoisomerization alters the affinity between the polymers and DNA, enabling precise spatiotemporal control over coacervate formation and dissolution (Figure 1b).

The researches described above allow the formation of single-phase coacervates. However, subcellular coacervates typically contain multiple coexisting structural domains rather than a single-phase state.[4] For example, the membrane-free nucleolus,

composed of RNA and proteins, forms through the immiscible self-assembly of several liquid phases, which contain multiple compartments inside.[4,29] To gain further insight into the underlying mechanisms driving the formation of multiphase coacervates and to establish rules for coacervate phase coexistence, researchers have initiated the design and synthesis of coacervates with more complex structures. Jing et al. constructed biphasic DNA coacervates by using ssDNA, PLL, and quaternized dextran (Q-dextran).[24] In this system, the PLL/ssDNA phase acted as the membrane-free inner chamber, while the Q-dextran /ssDNA phase served as the surrounding medium (Figure 1c). Fraccia et al. dynamically regulated the formation of biphasic coacervates through light-mediated photoisomerization of azobenzene.[30] Moreover, Lu et al. developed a method for synthesizing coacervates with three or more phases by combining ssDNA with multiple pairs of polycations and polyanions (Figure 1d).[16] They observed that the formation of multiphase coacervates is favored if the interfacial tension between coacervates is lower than the interfacial tension between one of the coacervates and the surrounding dilute phase. This phenomenon is primarily driven by the differences in interaction strengths between oppositely charged polymers, which lead to disparate critical salt concentrations. These disparities in salt concentrations result in varying densities, ultimately making them immiscible within the multiphase coacervates. Furthermore, the critical salt concentration also affects the distribution of phases within the multiphase coacervates. Among them, the coacervates with the highest critical salt concentration typically have the highest (charge) density and lowest water content, which is usually located at the core of the multiphase coacervates. Mountain et al. generated two or three coexisting multiphase complex coacervate systems by using several sets of oppositely charged polyelectrolytes and observed that the order of polymer additions was critical in achieving coexisting liquid phases in some cases.[17] In addition, Mao et al. emphasized that differences in chain length, charge density, and hydrophobicity of oppositely charged polymers, as well as their mixing ratios, can cause immiscibility, which may ultimately contribute to the formation of multiphase coacervates.[31]

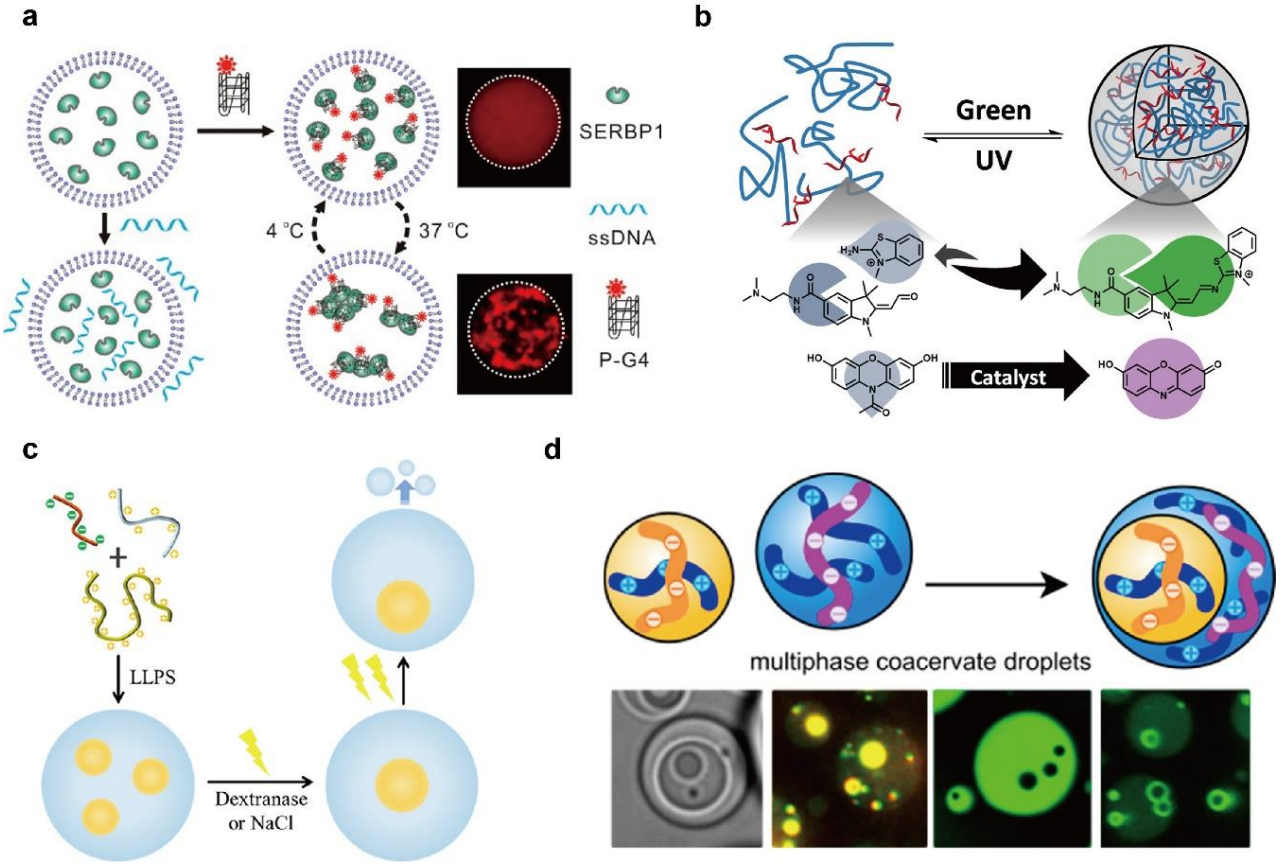

Figure 1 Formation of single-phase or multiphase DNA coacervates through electrostatic interaction-based strategy. (a) Schematic mechanism of liquid-liquid phase separation of G-quadruplex bound SERBP1.[19] Copyright © 2021, American Chemical Society (b) Light-controlled formation and disassembly of DNA coacervates formed from a complex of PLL and AAP-conjugated ssDNA.[28] Copyright © 2021 The Authors. (c) LLPS formation of biphasic coacervates by ssDNA, PLL and Q-dextran.[24] Copyright © 2020, American Chemical Society. (d) Formation of two/three-phase DNA coacervates.[16] Copyright © 2020 American Chemical Society.

In addition to the number of coacervate phases, the transition between liquid and solid phases can be regulated in a specific way. Vieregg et al. discovered that the phase state of the resulting complexes was governed by the hybridization state of the nucleic acids.[32] As illustrated in Figure 2a, when DNA with different hybridization states was mixed with PLL, double-stranded DNA (dsDNA) with hybridization ratios exceeding 40% formed irregular solid precipitates, whereas ssDNA formed spherical coacervate structures. A similar phenomenon was also observed when using RNA.[33] This phenomenon can be attributed to the characteristics of dsDNA, which exhibits higher charge density, greater rigidity, and increased hydrophilicity compared to ssDNA. These characteristics hinder the formation of coacervates with a loose interior and are more likely to result in solid precipitates. Based on this, Jing et al. introduced complementary strands to the coacervate formed by PLL and ssDNA.[34] They observed that when the concentration of complementary ssDNA was low, it first interacted strongly with the surface of the PLL/ssDNA coacervate, resulting in the formation of a gel-like membrane structure. However, when the concentration of complementary ssDNA was higher, it entered the coacervates. Due to the osmotic pressure, vacuoles were formed within the coacervates, pushing the

PLL/ssDNA towards the membrane (Figure 2b). Wang et al. investigated the influence of charge density on the phase state of the coacervate.[35] Subsequently, Shakya et al. employed DNA/PLL coacervates to investigate the effect of DNA flexibility on LLPS (Figure 2c).[36] Even for ssDNA, enhancing rigidity by increasing the number of adenine bases decreases the probability of LLPS. Additionally, adding free ATP to the solution leads to competitive interactions between ATP and dsDNA with cationic polymers, which reduces the strength of the interaction between dsDNA and the cationic polymer, thereby promoting LLPS. Besides, the solid precipitate formed by dsDNA is dynamic and can transform into a liquid coacervate by adjusting the concentration of salt ions and temperature in the solution. Vieregg et al. emphasized that high concentrations of salt ions can neutralize some of the negative charges and reduce the strong electrostatic attraction between dsDNA and PLL, facilitating the LLPS of dsDNA/PLL into a liquid coacervate with a loose interior.[32] Specifically, the transition from precipitate to coacervate occurs within a narrow range of salt concentration (500-700 mM), which depends on the length of the polymer and DNA sequence. Based on this, Fraccia and Jia et al. designed a short dsDNA with only 12 base pairs and mixed it with PLL to obtain coacervates that avoided precipitation (Figure 2d).[37,38] Besides, Liu et al. regulated the electrostatic interaction strength between the ATP-binding aptamer and PLL by adding ATP or applying an electric field to facilitate the release of ATP, thereby modulating the transition between precipitates and coacervates (Figure 2e).[39]

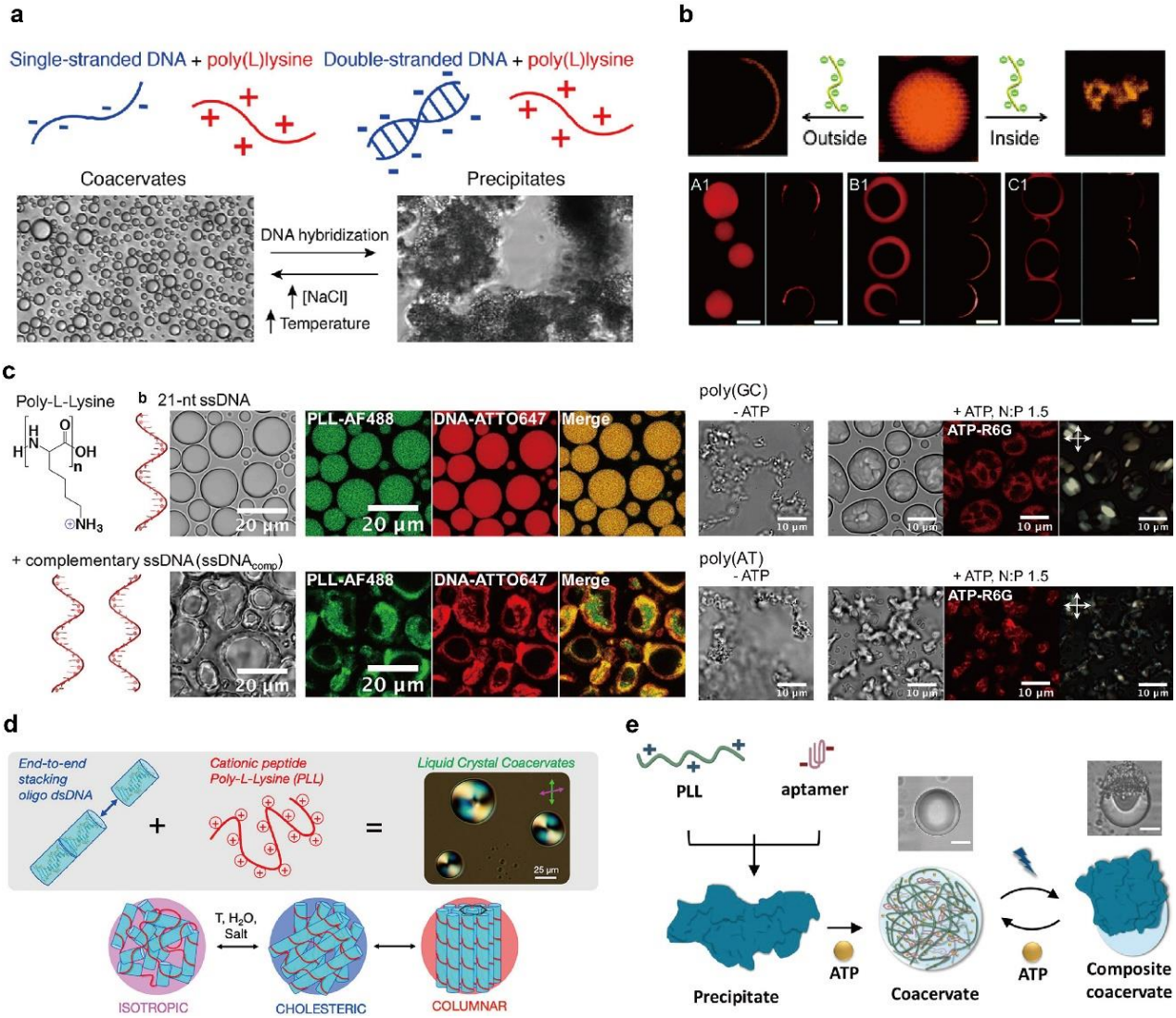

Figure 2 The relationship between the phase state of DNA coacervates and the hybridization state of DNA. (a) The phase of the complexes is controlled by the hybridization state of the DNA, with dsDNA forming solid precipitates while ssDNA forms liquid coacervates.[32] Copyright © 2018 American Chemical Society. (b) The state of DNA coacervates is controlled by hybridization.[34] Copyright © 2020, The Royal Society of Chemistry. (c) The role of DNA flexibility and ATP competition in LLPS.[36] © 2018 Biophysical Society. (d) DNA coacervates formed by short dsDNA.[37,38] Copyright © 2020, American Chemical Society. (e) DNA coacervate-precipitates state transition is controlled by adding ATP or releasing ATP with an electric field.[39] Copyright © 2022, American Chemical Society.

Although the electrostatic interaction-based synthesis pathway of DNA coacervates needs only simply mixing DNA with polycations, which is rapid and does not require expensive equipment or complex procedures, this strategy still has some drawbacks that limit the potential applications of DNA coacervates. Firstly, the single-stranded and double-stranded states of DNA may influence the morphology of the coacervates, making it difficult to fully exploit the programmability of DNA to expand the functionality of the coacervates. Secondly, membrane-less DNA coacervates formed via electrostatic interactions are susceptible to disruption by factors such as ions or other charged species in the reaction system, which limits their application in complex environments, such as in vivo conditions. Besides, due to the high DNA concentration required for synthesizing DNA coacervates and

the associated costs, the large-scale production of coacervates using DNA and cationic polymers remains challenging. To address this issue, salmon sperm DNA, known for being inexpensive, plentiful, and readily accessible, has been extensively employed in the synthesis of DNA coacervates. Liu et al. successfully prepared coacervates by directly mixing salmon sperm ssDNA and DEAE-dextran in a specified ratio.[40] In addition to using ssDNA, they also constructed coacervates using salmon sperm dsDNA by adjusting the experimental conditions, such as the ratio of reactants, ionic concentration, and pH.[41]

2.2. DNA hybridization-based strategy

The strict Watson-Crick base pairing rule enables the accurate prediction of DNA self-assembly based on precisely designed sequences, facilitating the construction of higher-order structures, such as micrometer-sized DNA hydrogel,[42,43] nanosized DNA polyhedron,[44,45] and DNA origami,[46-48] which opens up more possibilities for the formation of DNA coacervates. In addition to the traditional method of forming coacervates through electrostatic interactions between substances with opposite charges, Biffi et al. were the first to construct programmable DNA coacervates by modulating the phase behavior of DNA nanostructures.[49] These coacervates are composed of X- or Y-shaped DNA motifs, which undergo phase separation upon hybridization to create DNA-enriched phases. As illustrated in Figure 3a, DNA motifs are formed by annealing and self-assembly of three or four distinct ssDNA oligonucleotides. These ssDNA hybridize to form X- or Y-shaped motifs, each comprising three or four arms that converge at a junction. At the distal end of the junction, the tails of each dsDNA arm are terminated with ssDNA sequences of equal length. These tailed ssDNA sequences typically consist of palindromic sequences, acting as sticky ends. The sticky ends facilitate hybridization between disparate DNA motifs, which in turn leads to the formation of DNA-poor and DNA-rich phases through LLPS, ultimately forming DNA coacervates.[49-51] The formation of coacervates based on DNA hybridization has been extensively studied.[50-57] Agarwal et al. developed a method to control the active and inactive states of DNA motifs through UV irradiation, which triggers the formation of DNA coacervates. [58] They designed an improved three-arm DNA motif with one arm protected by a photocleavable (PC) domain, effectively reducing its valency to two and preventing coacervate formation. Upon exposure to UV radiation, the protective domain is cleaved, increasing the valency to three and facilitating coacervate formation. This method allows the regulation of coacervate formation by adjusting the intensity and distance of irradiation, offering a "remote" mechanism for controlling LLPS without altering the ionic conditions, temperature, or composition of the sample.

It is worth highlighting that DNA coacervates formed by self-hybridization of DNA motifs are unstable structures due to the reversibility of DNA hybridization. These structures can exhibit a transition between the gel and liquid states, with their transitions influenced by temperature. Sato et al. provided a detailed discussion of this process, as illustrated in Figure 3b.[55] It was observed that DNA motifs exist in a dispersed state at high temperatures. As the temperature gradually decreases, LLPS occurs at a certain threshold temperature, resulting in the formation of DNA coacervates with fluidity. Fluorescence recovery after photobleaching (FRAP) experiments showed that the fluorescence of the bleached region recovered rapidly, indicating the presence of a liquid network inside. Upon further cooling to room temperature, the liquid DNA coacervate transformed into a non-flowing DNA gel. The FRAP experiments revealed that the bleached region did not recover in the corresponding time, indicating a static internal structure.[54] This process involves two key structural transition temperatures: the temperature at which dispersed DNA nanostructures transform into DNA coacervates (T_d) and the temperature at which DNA coacervates transform into DNA gels (T_g). The values of these temperatures, as well as the internal fluidity of the DNA coacervate, depend on the sequence design of the DNA motifs,[50,52,55] the number of branches (sticky ends) in the DNA motifs,[49,53,55,57] and the ionic strength of the reaction system.[59,60] The following sections will discuss the influence of these factors on the morphology of DNA coacervates.

Firstly, the design of arm lengths and sticky ends of DNA motifs is crucial for the morphology of the coacervates. It has been demonstrated that increasing the arm length of DNA motifs accelerates the formation of DNA coacervates and results in larger sizes (Figure 3f).[61] Besides, Sato et al. investigated the impact of sticky ends on coacervates and observed that T_d and T_g increased as the number of bases at the sticky ends increased (Figure 3e).[55] Through FRAP experiments and viscosity tests, they further revealed that as the number of sticky end bases increased, the mobility of DNA coacervates decreased.[62] Notably, the ratio of viscosity to surface tension of coacervates differed significantly, with a factor of 28 between the 12 nt and 4 nt designs. Nguyen et al. proposed that, in addition to optimizing the number of bases in the sticky ends, an additional adenine base should be incorporated near the dsDNA ends as a “flexible base” that remains unpaired during the hybridization of DNA motifs arms (Figure 3c).[50] The design of this unpaired base is crucial for the self-assembly of DNA motifs into coacervates, as it increases the flexibility of the motifs and reduces the interactions between neighboring two phases. These properties promote the formation of liquid coacervates instead of gels. However, Lee et al. discovered that introducing an ssDNA gap in the middle of each arm significantly enhanced the flexibility of DNA motifs, which in turn inhibited the formation of coacervates (Figure 3d).[51] The introduction of a gap of six nucleotides resulted in the absence of any observed coacervate generation.

Secondly, the number of branches in the DNA motif is closely related to the formation of DNA coacervates. Biffi et al. designed coacervates with a branch number of 3 or 4 and found that both T_d and T_g increased as the number of branches in the DNA motif increased, with T_g increasing significantly more than T_d.[49] Sato et al. extended this study by showing that when the number of branches in the DNA motifs was increased from 3 to 6, the temperature at which coacervates transformed into dispersed structures rose by 10°C, and the temperature at which the DNA gel transformed into the DNA coacervate increased by 25°C (Figure 3e).[55]

Finally, the fluidity of DNA coacervates is influenced by the ionic strength of the reaction system, as ionic strength affects the electrostatic repulsion between the negatively charged phosphate backbone of DNA. Jeon et al. investigated the effect of salt ion concentration and found that the viscosity within DNA coacervates increased with rising concentrations of NaCl.[60] Specifically, as the NaCl concentration increased from 0.25 M to 1 M, the viscosity rose by more than threefold, indicating that higher salt ion concentrations reduce the fluidity of DNA coacervates at the same temperature (Figure 3g).

In recent years, researchers have expanded beyond classical DNA coacervates formed through self-hybridization of DNA motifs to include those featuring cholesterol labels at their ends. Leathers and Walczak et al. introduced cholesterol labels at the ends of DNA motif core sequences, which facilitated the formation of core coacervates driven by the hydrophobic effect of cholesterol, allowing the exposed sticky ends to hybridize with other DNA motifs and enabling the design of customizable multilayer shell structures around the coacervates.[63,64]

Moreover, multivalent interactions between long DNA sequences can also drive LLPS to construct DNA coacervates. Deng et al. reported an ATP-driven synthesis of membrane-free DNA coacervates.[65] Specifically, the ATP-driven T4 DNA ligase links two complementary DNA monomers to form a sequence-defined

functionalized nucleic acid polymer (sfNAP). Multivalent interactions between the two sfNAPs then trigger the formation of DNA coacervates via LLPS. The customized design of the sfNAP side chain sequence can adjust the internal fluidity of the coacervates. In addition to using ATP to trigger these multivalent interactions, Liu et al. constructed a self-regulated coacervate system with a tunable lifetime by integrating DNA- and RNA-triggered strand displacement reactions with RNase H-mediated degradation. This approach enables controlled assembly and disassembly of coacervates.[66]

In summary, the formation of DNA coacervates through self-hybridization of DNA motifs is a promising strategy. It allows for the formation of multiple orthogonal DNA coacervates in solution through the design of DNA sequences. These different types of DNA coacervates are immiscible with each other, enabling the independent occurrence of various reactions, which facilitates the design of complex reactions and broadens the application potential of DNA coacervates. Furthermore, this strategy allows for the controllable regulation of DNA coacervate formation, as well as the fusion and dissociation between different types of DNA coacervates, providing more possibilities for their applications. However, a limitation of this strategy is that the DNA coacervates formed are temperature-dependent, exhibiting fluidity only at certain temperatures. This drawback imposes strict requirements on imaging instruments and experimental conditions and limits the application scenarios.

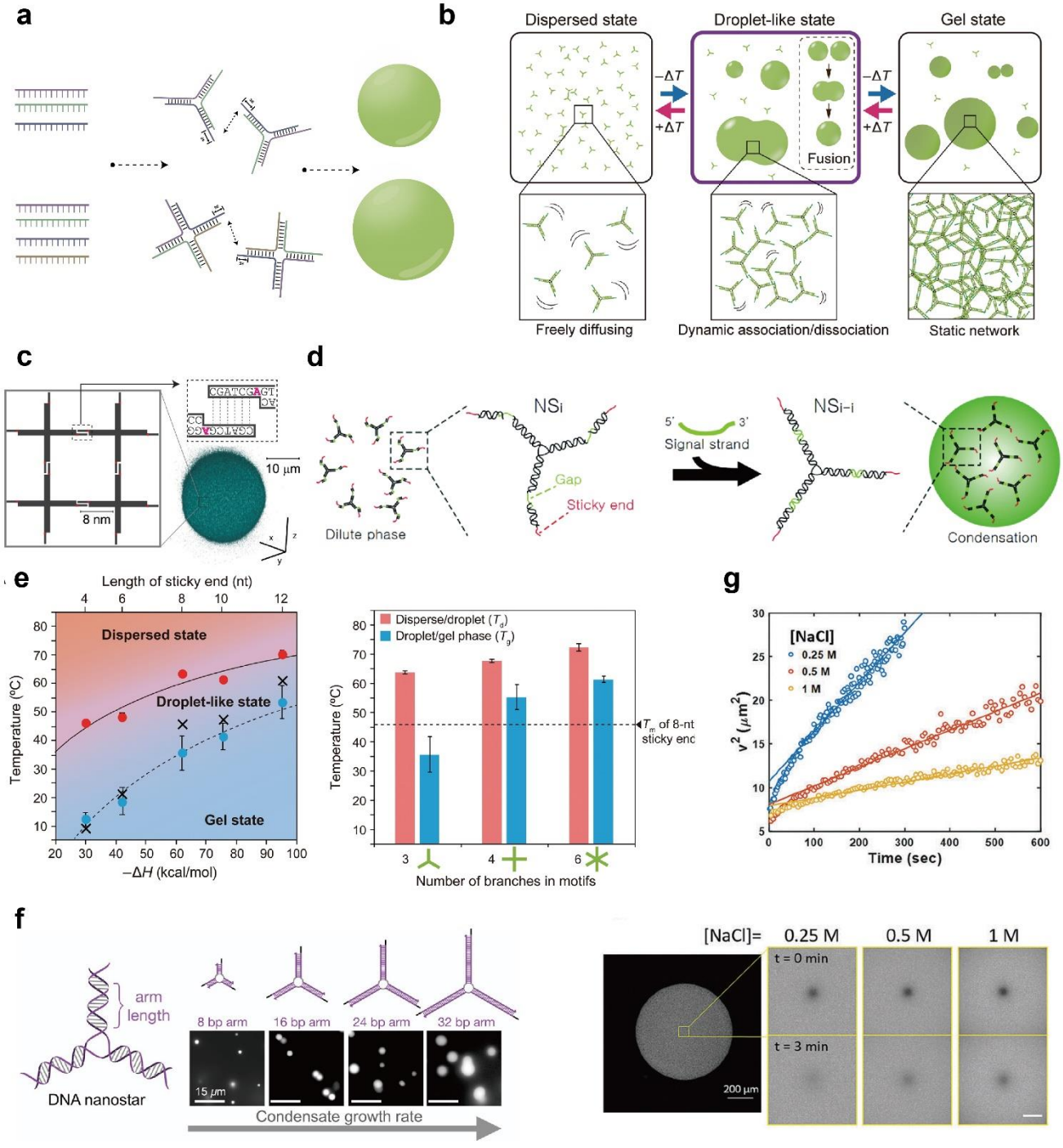

Figure 3 Formation of DNA coacervates through DNA hybridization-based strategy (a) Schematic mechanism of coacervates Formed by DNA Hybridization-Driven LLPS. (b) The fluidity of DNA coacervates is affected by temperature.[55] Copyright © 2020, The American Association for the Advancement of Science. (c) An unpaired "flexible base" needs to be introduced at the end of the dsDNA arm.[50] Copyright © 2019, American Chemical Society. (d) Construction of

DNA motif with varying degrees of flexibility by introducing single-stranded gaps of different lengths in dsDNA arms.[51] Copyright © 2021, Royal Society of Chemistry. (e) Relationship between the number of branches of DNA motif with the structural transition temperature of DNA coacervates.[55] Copyright © 2020, The American Association for the Advancement of Science. (f) Relationship between the arm length of DNA motif with the growth rate of DNA coacervates.[61] Copyright © 2022, American Chemical Society. (g) The relationship between the fluidity of DNA complexes and the ionic strength within the reaction system.[60] Copyright © 2018, Royal Society of Chemistry.

2.3. Adenine-rich strand-based strategy

A-rich ssDNA strands have been found to undergo phase separation upon heating. In 2018, Merindol et al., for the first time, combined reversible phase separation of A-rich ssDNA strands with hybridization to construct all-DNA coacervates with core-shell structures.[67]

As illustrated in Figure 4a, unlike the mechanism of DNA coacervate formation based on the hybridization of branched DNA, this core-shell structured DNA coacervate is formed from long ssDNA produced by rolling circle amplification (RCA) of A-rich sequences, which spontaneously undergo LLPS at high temperatures. Thymine-rich (T-rich) ssDNA sequences were also added to stabilize the coacervate during cooling and prevent its dissolution and dispersion. As the temperature was gradually increased to the cloud point temperature (T_{cp}), the A-rich sequence underwent LLPS to form a coacervate. Upon further temperature increase to the melting temperature (T_m), the T-rich sequences were expelled to the exterior of the coacervate. During cooling, when the temperature dropped below T_m, the expelled T-rich sequences rapidly hybridized at the boundary of the coacervate before they dissolved, forming an immobile crosslinked shell layer. This layer prevents further dissolution of the internal coacervate by stabilizing its kinetics. Furthermore, FRAP experiments confirmed that the product is a caged coacervate of liquid DNA encapsulated in a solid-state DNA gel.[67] Liu et al. described the adenine-rich strand-based LLPS process as a two-stage process, which involves two temperature changes (Figure 4b).[68] First, a stable nucleus, significantly smaller than the optical diffraction limit, forms at the critical temperature T_1, referred to as the nucleation temperature. Subsequently, the temperature is increased to the critical temperature T_2, referred to as the growth temperature, leading to the rapid formation of micrometer-sized coacervates through growth and aggregation. The structural properties of such core-shell structured all-DNA coacervates are also influenced by several factors, including sequence length, concentration,[67] and ionic species.[68]

Firstly, the T_{cp} increases as the length of the RCA product decreases, which consequently affects coacervate formation. Merindol et al. demonstrated that the critical length for phase separation is 75-100 nt at 50 mM Mg^{2+}.[67]

Secondly, the concentration of the DNA strand significantly influences the particle size of the coacervates. As DNA concentration increases, the size of the DNA coacervates also increases. Merindol et al. found that the particle size increased threefold when the DNA concentration was raised from 0.1 g/L to 0.9 g/L.[67]

Finally, the stability of DNA coacervates is influenced by the ionic species. Liu et al. revealed that Ca^{2+} can induce the formation of more stable DNA coacervates without any additional assistance. In contrast, when using Mg^{2+}, the formation of a crosslinked shell structure on the surface is required to stabilize reversible liquid coacervates at high temperatures (Figure 4c-i).[68] This is because A-rich sequences have a higher binding affinity for Ca^{2+}, and this effect is more pronounced at high concentrations of DNA strands.[69-71] As a result, there is a decrease in strand mobility in the coacervate state, leading to the permanent kinetic capture of the coacervates. This was validated by FRAP experiments, which showed that Ca^{2+}-induced DNA coacervates exhibit a slower recovery rate of internal fluorescence compared to those induced by Mg^{2+}. Interestingly, in addition to A-rich sequences, Ca^{2+} can also induce T-rich sequences to form stable DNA coacervates. (Figure 4c-ii).

Similar to DNA hybridization-based strategies, the A-rich chain-based approach allows for the coexistence of multiple orthogonal DNA coacervates in solutions. Furthermore, the core-shell structure enables modular design in different regions. The external cross-linked shell also provides protection against external environmental interference, thereby maintaining the stability of the core-shell structure in buffer solution. Additionally, the internal environment remains in a liquid state, exhibiting minimal sensitivity to temperature fluctuations during experiments. However, to achieve multifunctionality, the design of such DNA coacervates is relatively complex, as it is essential to avoid unnecessary hybridization between strands. Moreover, there are certain limitations in the synthesis process, such as the requirement for high concentrations of enzymes and ions, the complex and time-consuming preparation process, and the associated higher costs.

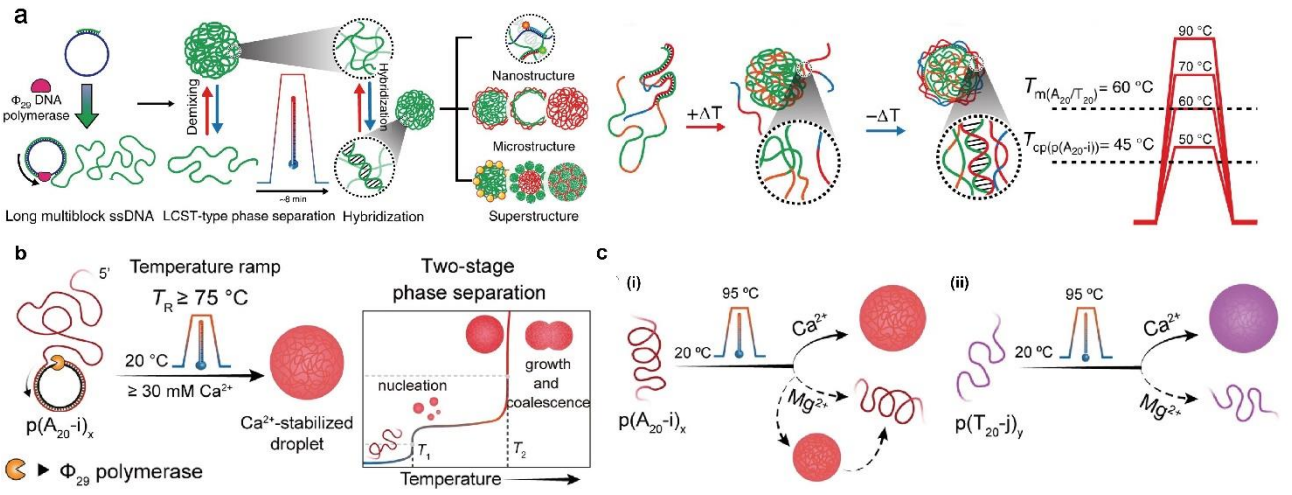

Figure 4 Formation of DNA coacervates through adenine-rich strand-based strategy. (a) Schematic mechanism of DNA coacervate formation by temperature-regulated LLPS of RCA products.[67] Copyright © 2018, The Author(s). (b) A two-stage process for the formation of DNA coacervates from RCA synthesis products in a Ca^{2+} environment.[68] Copyright © 2022 The Authors. Angewandte Chemie International Edition published by Wiley-VCH GmbH. (c) DNA coacervates Irreversible phase separation under Ca^{2+} conditions and reversible phase separation under Mg^{2+} conditions.[68] Copyright © 2022 The

3. Biomimetic Applications of DNA Coacervates

To gain insights into the fundamental mechanisms of life processes and cell function, an increasing number of researchers are employing a bottom-up approach to construct artificial cells aimed at mimicking cellular functions, such as cell motility,[72,73] feeding,[74-77] information processing,[78] and signaling.[79] Due to the high dynamic adjustability, coacervates can rapidly respond to changes in environmental conditions, therefore can effectively mimic various dynamic processes of biological cells, such as protein interactions, signal transduction, and molecular exchange. Compared to coacervates formed by proteins, peptides, or polycations and polyanions, DNA coacervates have superior programmability and allow for more complex bionic applications through rational sequence design.[80] This section will present the bionic applications of DNA coacervates in mimicking single-cell behavior, intercellular and intracellular information exchange, and tissue-like formation.

3.1. Mimicry of cell morphology

3.1.1. Mimicry of cell growth

The processes of cell growth and cell division into two nearly identical copies are unique hallmarks of living organisms.[81] By leveraging the flexible design of DNA sequences and the dynamic adjustability of DNA coacervates, the process of cell growth can be mimicked through the regulation of fusion between coacervates. Wilken et al. described the dynamics of DNA coacervate formation.[82] They noted that coacervates formed by electrostatic interactions exhibit the same dynamic characteristics compared to those formed via DNA hybridization. The growth of coacervates can be regulated through the design of a DNA motif. Agarwal et al. demonstrated that the growth rate of DNA coacervates synthesized via DNA hybridization depends on both the size and concentration of the DNA motifs.[61] Their studies indicate that the average diameter of DNA coacervates increases with higher concentrations of DNA motifs, and coacervates generated from DNA motifs with longer arms grow more rapidly. However, according to the result of Agarwal et al., although the size of the motif affects the growth rate of DNA coacervates, it does not stably control the size of the coacervates. Furthermore, this study did not investigate the relationship between the length of the sticky ends of the motif, solvent conditions and the coacervates growth process, which still needs to be further explored by researchers. The study by Sato et al. showed that when two DNA coacervates collide in solution via Brownian motion, fusion and growth of coacervates can occur within a few minutes due to the liquid nature of DNA coacervates and the palindromic design of the sticky ends of DNA motifs (Figure 5a).[62] Since DNA is an anionic polymer, two different motifs with non-complementary sticky ends cannot hybridize due to charge repulsion, which consequently prevents coacervate fusion and growth. To address this issue, Sato et al. developed a six-connector S-motif that can simultaneously bind to other DNA motifs from two different sticky ends, thereby facilitating cell-like fusion and growth between distinct coacervates (Figure 5b).[55]

In addition to mimicking cell behavior through sequence-triggered responses, alternative methods have also been employed. Samanta et al. encapsulated artificial metalloenzymes (ARM) within the coacervates formed by A-rich ssDNA phase separation.[83] As demonstrated in Figure 5c, these enzymes catalyze the conversion of diene substrates Biot-Ru into self-reporting products that can interact with DNA in the shell layer. Specifically, the enzyme Biot-Ru facilitates the release of the naphthalene precursor of hydroxycoumarin, which can be embedded in the DNA duplexes of the shell layer, particularly at the A/T base pair. This weakens dsDNA interactions, increases the mobility of the shell layer, and ultimately causes the coacervates to swell and grow. This method converts non-DNA signals into downstream functional and morphological changes, such as cell growth, division, and fusion, through catalytic reactions. Furthermore, Kumar et al. improved the growth of DNA coacervates through enzyme-catalyzed reactions.[72] Specifically, catalase (CAT) or glucose oxidase (GOx) was encapsulated during the synthesis of DNA coacervate and wrapped around their periphery with organoclay to increase membrane elasticity. Upon the addition of H_2O_2, the oxygen produced by enzymatic catalysis causes the coacervate to swell, expanding to six times its original volume before the membrane ruptures. The GOx-mediated glucose-to-gluconate conversion consumes oxygen, which in turn causes the contraction of the DNA coacervates, completing a reversible cycle.

3.1.2. Mimicry of cell division

Leveraging the programmability of DNA, researchers can mimic cellular life processes in response to stimuli through precise sequence design and external regulation. For example, behaviors such as cell division can be controlled by incorporating trigger sequences. Maruyama et al. introduced a toehold sequence between the core of the six-connector S-motif and the sticky end sequence, enabling S-motif to split into two parts via toehold-mediated strand displacement (TMSD) in the presence of ssDNA division trigger factors.[84] This process resulted in the division of large coacervates into smaller ones (Figure 5d). Sato et al. incorporated RNA sequences into the core region of S-motif, termed chimerized-S-motif (CS-motif).[55] The enzymatic reaction of RNase A caused the CS-motif to split into two “Y parts”, resulting in the loss of its cross-bridging capability. Ultimately, complete fission into two or three coacervates was observed (Figure 5e-i). Additionally, through complementary base pairing and biotin-streptavidin (SA) interactions, different DNA coacervates are capable of selectively capturing cargo molecules (Figure 5e-ii). Tran et al. replaced the core region of S-motif DNA with RNA or a PC linker to control the division of coacervates using RNase A or light, thereby mimicking the process of cellular division.[56] Besides, the reaction rate can be accelerated by reducing the concentration of salt ions and increasing the reaction temperature.

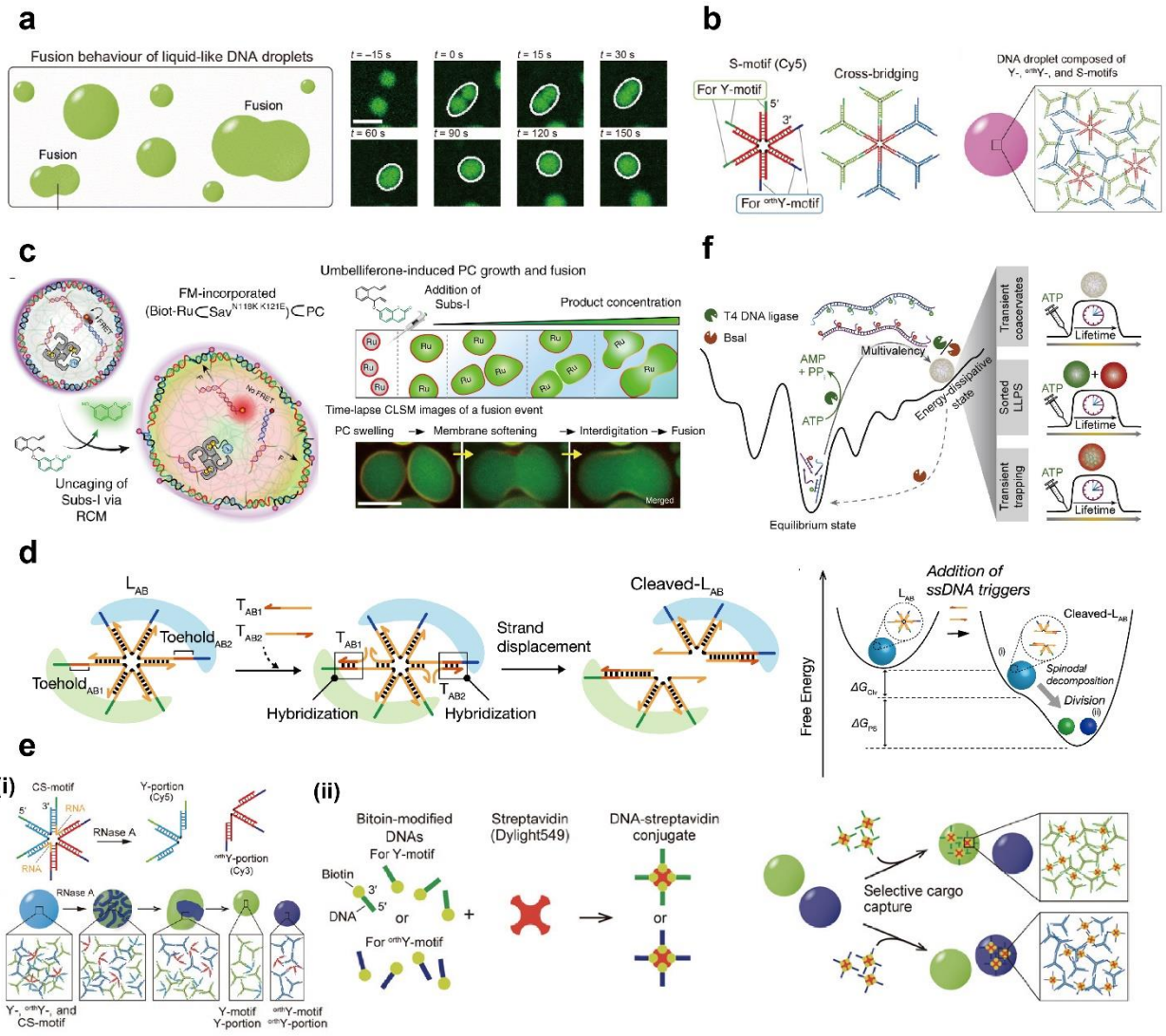

Figure 5 DNA coacervates are used to mimic cell growth and division. (a) DNA coacervates fusion growth.[62] Copyright © 2018, Royal Society of Chemistry. (b) Promoting fusion of non-complementary NSs by six-connector S-motif.[55] Copyright © 2020, The American Association for the Advancement of Science. (c) Triggering DNA coacervate splitting by TMSD.[84] Copyright © 2024, The Author(s). (d) Triggering DNA coacervate division by light and RnaseA.[84] Copyright © 2020, The American Association for the Advancement of Science. (e) The enzyme catalyzes the decomposition of the diene substrates Biot-Ru to produce a shell-embedded substance that promotes morphological changes in DNA coacervates.[83] Copyright © 2020, The Author(s), under exclusive license to Springer Nature Limited. (f) ATP-driven multivalent interactions to form DNA coacervates by LLPS.[65] Copyright © 2020 Elsevier Inc.

3.1.3. Mimicry of cell cycle

To mimic the cell cycle, a time-adjustable cellular behavior model was developed. Maruyama et al. introduced a substantial amount of inhibitory single-stranded RNA (ssRNA) into the coacervate system formed by the S-motif nanostructure.[84] ssRNA can hybridize with the division trigger DNA to inhibit its release. Only when RNase A degrades the inhibitory ssRNA can the division trigger DNA be released, allowing the coacervate to undergo a cell-like division process. This results in a delayed cutting time of the S-motif, thereby enabling temporal control over the division time of DNA coacervates by adjusting the amount of inhibitory ssRNA. Deng et al. controlled the timing of growth and division of DNA coacervates by varying ATP levels, similar to a programmable cell cycle.[65] As illustrated in Figure 5f, ATP provides the energy necessary for T4 DNA ligase to facilitate the formation of a long DNA strand and promote the formation of DNA coacervates through LLPS, which gradually increases in size over time. When ATP is depleted within the system, the coacervate undergoes a process of splitting and disassembly in the presence of the nucleic acid endonuclease BsaI, thereby mimicking the stages of a cell cycle. Saleh et al. also designed restriction endonuclease cleavage sites on the arms of DNA motifs that allow the enzyme to penetrate DNA coacervates, driving DNA degradation and forming relatively dilute interiors within coacervates. These coacervates undergo multiple cycles of growth, bursting, and regeneration due to osmotic pressure differences.[85] In a subsequent study, the same group proposed that these growth, bursting, and regeneration processes could also facilitate cell-like motility.[86]

3.2. Mimicry of cell metabolism

Cell metabolism is fundamental to sustaining the basic life activities of an organism. Mimicking cell metabolism represents a sophisticated application of synthetic cell biomimicry. The liquid and macromolecule crowded environment within the DNA coacervates provides an appropriate setting for metabolic reactions and sometimes can accelerate the metabolic processes. Therefore, DNA coacervates are regarded as micro-reactors for mimicking cellular metabolism. Deng et al. successfully mimicked the in vitro transcription process (IVTx) by encapsulating a DNA template that encodes the Spinach2 aptamer sequence within a

DNA coacervate formed by electrostatic interactions.[87] This approach effectively mimicked the RNA production of the nucleus in the presence of polymerase (Figure 6a). Also, specific template sequences can be encapsulated in different regions through precise design of the DNA sequence. As illustrated in Figure 6b, Leathers et al. utilized complementary base pairing and hydrophilic interactions of cholesterol-modified tetradentate DNA nanostructures (TDNs) to construct DNA coacervates with a core-shell structure and localize functional elements in different regions.[63] The core region encodes the DNA template and T7 RNA polymerase promoter sequences, while the shell region contains complementary sequences, creating an active cell nucleus capable of producing fluorescent RNA aptamers and a storage shell for gradual product accumulation. Malouf et al. combined the generation of fluorescent RNA aptamers with the regulation of coacervate morphology.[88] They found that, in contrast to TMSD, which caused the collapse and disintegration of the coacervates, RNA production in the nuclear region combined with the fluorophore DFHBI increased transient osmotic pressure, which in turn led to the expansion of the nuclear periphery and the restoration of cellular morphology (Figure 6c). Enzymatic cascade reactions can also be used to mimic cellular metabolism. As illustrated in Figure 6d, Chen et al. encapsulated GOx, horseradish peroxidase (HRP) and CAT within the coacervates and utilized H_2O_2 for polydopamine (PDA) synthesis.[41] GOx catalyzed the generation of H_2O_2, while CAT acted as a competing enzyme to deplete H_2O_2, thereby regulating product synthesis. Moreover, the crowding effect within the coacervates could significantly accelerate the biological reaction rate, thereby increasing the quantity of product generated at the same time. For example, encapsulating ribozymes in DNA coacervates enhances the conformational stability of the ribozyme-substrate complex, leading to a substantial increase in the cleavage rate of the ribozymes in the presence of Mg^{2+}.[40]

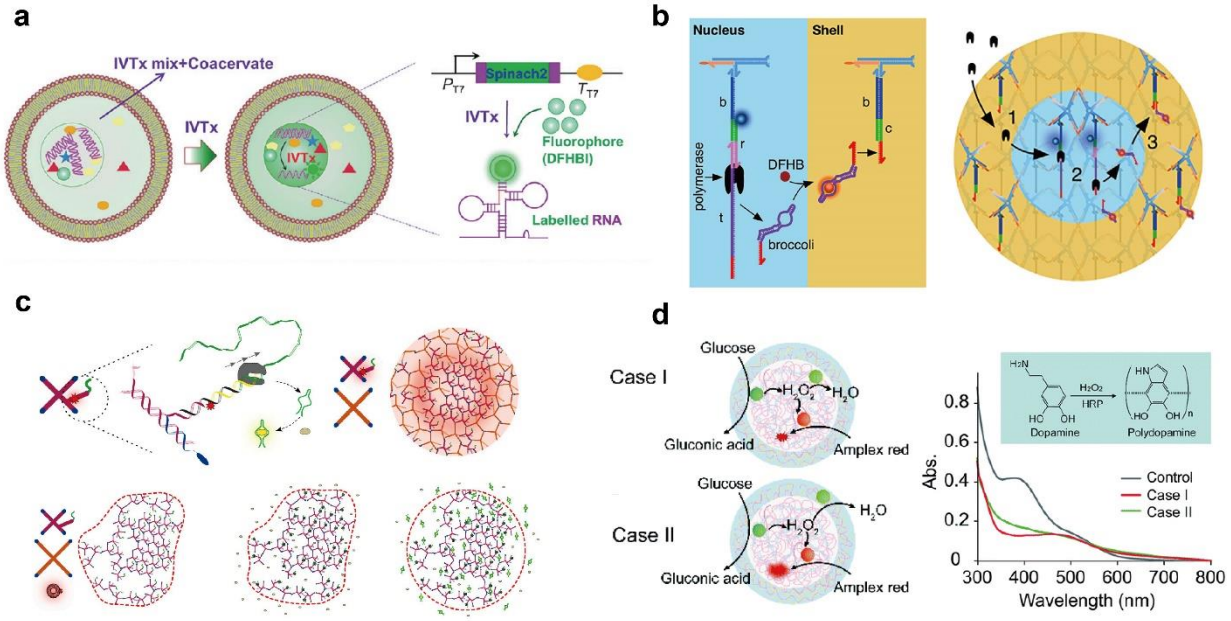

Figure 6 DNA coacervates are used to mimic cellular metabolism. (a) Schematic mechanism of the IVTx process within DNA coacervates.[87] Copyright © 2017 The Authors. Published by Wiley-VCH Verlag GmbH & Co. KGaA. (b) Control of the spatial distribution of IVTx products in DNA coacervates.[63] Copyright © 2022 The Authors. (c) Recovery of TMSD-induced morphological changes in DNA coacervates by IVTx.[88] Copyright © 2023 The Author(s). Published by Elsevier Inc. (d) Regulation of PDA synthesis by enzymatic cascade reactions.[41] Copyright © 2020, Royal Society of Chemistry.

3.3. Mimicry of intra/intercellular communication

The exchange and transduction of matter, energy and information among cells are crucial for the survival of organisms.[89] DNA coacervates as a feasible and programmable bionic platform, have been implemented in the mimicry of intracellular and intercellular communication by encapsulating artificial signaling systems. The light-triggering strategy provides a spatially regulated way to mimic intra- and intercellular communication. Zhao et al. realized the bidirectional transport of signals between organelle-like coacervates via a light-activated switch.[90] Two distinct DNA coacervates were prepared by LLPS within water-in-oil droplets. Both hairpin DNA and dsDNA sequences containing azobenzene were designed to undergo trans/cis photoisomerization under visible/ultraviolet (Vis/UV) irradiation. Release in cis and capture in trans of complementary DNA strands allowed the reversible transfer of signaling molecules between DNA coacervates, thus mimicking controlled unidirectional and bidirectional communication between subcellular compartments (Figure 7a). Martin et al. used dsDNA and light-responsive azobenzene cations (trans-azobenzenetrimethylammonium bromide; trans-azoTAB) to induce LLPS and generate DNA coacervates that could be disassembled and reassembled within seconds under UV and blue light, facilitating the transfer of DNA signaling molecules between two coacervates (Figure 7b).[15] Although this strategy enables the light-activated transport of cargo molecules, the intercellular communication method that relies on the decomposition of donor cells is relatively uncommon in nature. Moreover, the decomposition of donor cells means that this strategy cannot realize repeated or reciprocal intercellular communication. In addition, Chen et al. established signaling communication between different protocells.[91] As shown in Figure 7c, DNA coacervates encapsulated with the GOx/CAT cascade functioned as the sender cell for H^+ signal release, while pH-activated artificial membrane receptor vesicles acted as the receiver cell. The DNA coacervates converted glucose input into H^+ output, activating receptor dimerization on the vesicles and triggering a subsequent fluorescence cascade and polymerization reaction inside, thereby creating a model for intercellular signal communication that mimics the signaling networks present in biological systems.

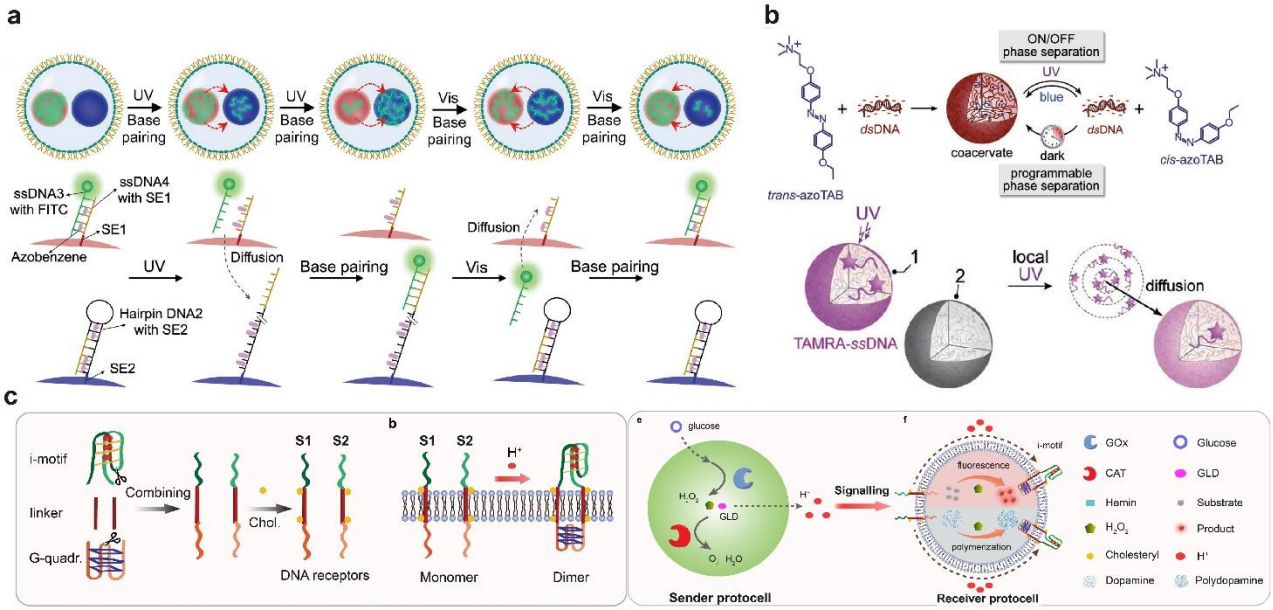

Figure 7 DNA coacervates are used to mimic cellular communication. (a) Light-driven unidirectional and bidirectional reversible communication between DNA coacervates.[90] Copyright © 2022 Wiley-VCH GmbH. (b) After disassembly of the coacervate formed by dsDNA and trans-azoTAB under UV, the DNA is delivered to another coacervate that does not contain trans-azoTAB.[15] Copyright © 2019 Wiley-VCH Verlag GmbH & Co. KGaA, Weinheim. (c) Signal communication between DNA coacervates and vesicles.[91] Copyright © 2023 Wiley-VCH GmbH.

3.4. Construction of membrane-bound DNA coacervates and proto-tissues

Using DNA coacervates to construct proto-tissues has attracted wide attention recently and lays the foundation for the ambitious goal of fabricating synthetic organs. However, DNA coacervates tend to aggregate and grow into larger coacervates to reduce total interfacial energy,[92] which poses a challenge in terms of their assembly into compact tissue structures. Therefore, it is necessary to construct membrane-bound DNA coacervates through hybridization, electrostatic and hydrophilic interactions. The coacervates formed by the A-rich strand as mentioned above can form a gel-like shell structure through hybridization.[67] Coacervates formed through electrostatic interactions typically possess longer cationic polymer chains, which give them net positive charges compared to those formed by DNA motifs. In earlier studies, fatty acids were commonly used to construct membrane-bound DNA coacervates.[93] However, the single-chain structure of fatty acids and their weak intermolecular interactions lead to inefficient encapsulation of the coacervate phase and low stability in the resulting membrane-bound microcompartments, which greatly limits the further application of membrane-bound DNA coacervates. Chen et al. employed negatively charged CM-dextran and positively charged DEAE-dextran to create layer-by-layer assemblies on the surface of a positively charged PDDA/DNA coacervate, resulting in a membrane-like structure (Figure 8a).[41] Moreover, phospholipids, the primary components of cell membranes with high biocompatibility and low immunogenicity, can endow phospholipid bilayer structure to coacervates. Liu et al. employed the hydrophilic head groups and hydrophobic tails of dioleoyl phosphatidylcholine (DOPC) to achieve stable encapsulation on the surface of coacervates, forming a membrane-layer structure (Figure 8b).[94] The use of dipalmitoyl phosphatidylcholine (DPPC) has further demonstrated the universality of this method (Figure 8c).[40] These strategies that utilize phospholipid molecules effectively address the limitations of previous approaches. In contrast to membrane-free coacervates, lipid-coated coacervates exhibit reversible hypo-osmotic swelling and hyper-osmotic contraction in response to changes in the surrounding osmotic pressure. As illustrated in Figure 8d, Zhang et al. utilized this hypo-osmotic swelling property to generate multi-chamber vesicles, resulting in increased volume and enhanced membrane permeability.[95] The increased membrane permeability improves transmembrane transport of substances, thereby triggering and amplifying artificial signaling cascades and endogenous enzyme reactions. Chang et al. generated membrane structures on the surface of coacervates using didodecyldimethylammonium bromide (DDAB). Under an electric field, molecules with different charges or sizes follow specific uptake pathways, producing distinct distributions within the coacervates.[96] Moreover, Liu et al. devised a synthetic cell inspired by cellular origin.[97] The membrane structure is primarily formed through the spontaneous self-assembly of hemoglobin-containing erythrocyte membrane fragments on the surface of DNA coacervate. The encapsulation of the erythrocyte membrane fragments provides a physical barrier for coacervates, minimizing contact between the coacervates and natural erythrocytes. This results in notable enhancements in hemocompatibility, increased efficiency of blood circulations, and prolonged circulation times (Figure 8e).

Coacervates with membrane-layered structures can form stable tissue-like structures. Merindol et al. used core-shell structured DNA coacervates to construct tissue-like structures.[67] Thousands of coacervates were bound together through hybridization of ssDNA modified on the gel shell to form millimeter-scale aggregates. Constructing synthetic proto-tissues driven by intercellular signaling is more attractive. Samanta et al. loaded DNAzymes into DNA coacervates.[98] Under exogenous input or mimicked intercellular communication, DNA signals can be converted into functional metabolites that are incorporated into the shell layer of the coacervates. Then, exposed palindromic sequences can drive multivalent interactions among the coacervates, resulting in the formation of tissue-like aggregates. The size of the tissue depends on the surface density of the palindromic sequences on the shell. An increase in this surface density will lead to a corresponding increase in tissue size (Figure 9a). Chen et al. proposed a model of coacervates that mimics the process of stimulus-triggered tissue formation with the internal encapsulation of GOx and $CaCO_3$.[99] In this model, the DNA coacervate functions as a synthetic cell micro-reactor, accelerating

the internal enzyme cascade reaction to promote the release of Ca^{2+} into the sodium alginate phase, which in turn triggers the tissue formation of native calcium alginate hydrogels (figure 9b). Subsequently, Liu et al. constructed tubular proto-tissue-like blood vessels with more complex structures.[94] As illustrated in Figure 9c, three DNA coacervates loaded with different materials were assembled into consecutive concentric modules by gel perfusion, resulting in the formation of a three-layer tubular model of native tissue vessels. Jeon et al. achieved the adhesion of membrane-free coacervates and the formation of tissue-like structures by designing the core sequence of DNA motifs.[52] When two motifs share the same core sequence, a "cross-linker" DNA structure is formed due to the imperfect self-assembly of motifs. Since the amount of "cross-linker" DNA structures is small, it leads to adhesion rather than fusion between DNA coacervates.

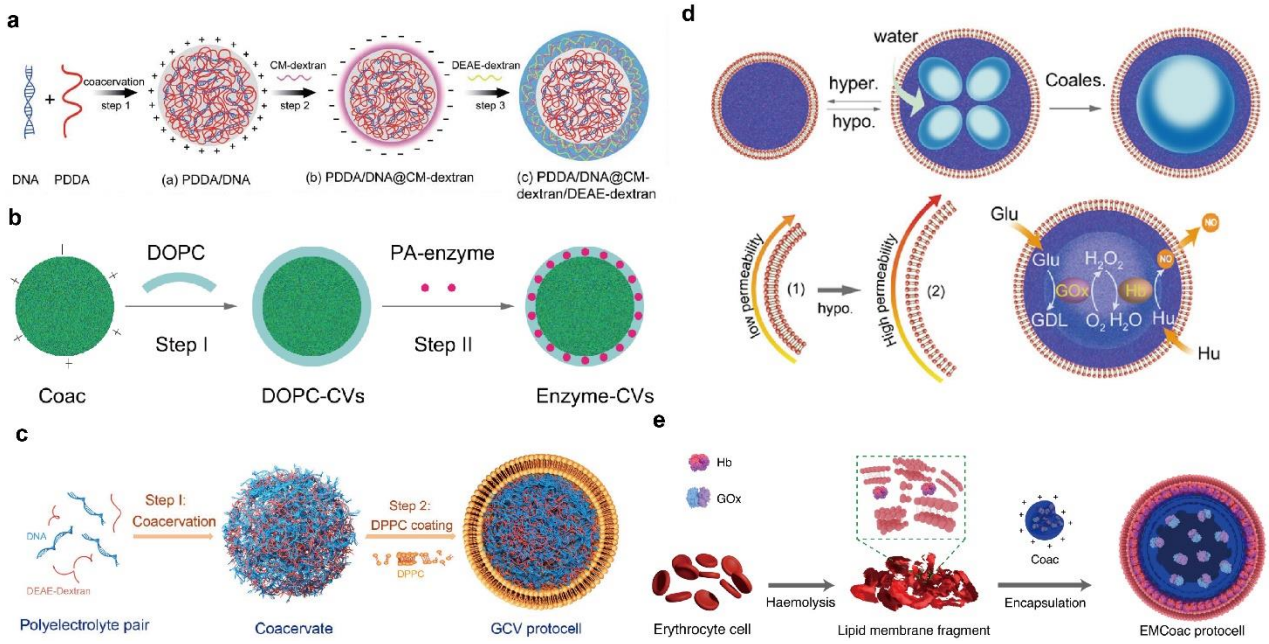

Figure 8 Construction of membrane-bound DNA coacervates. (a) Layer-by-layer assembly using negatively charged CM-dextran and positively charged DEAE-dextran in positively charged DNA coacervates, thereby forming membrane structures.[41] Copyright © 2020, Royal Society of Chemistry. (b) Formation of a phospholipid envelope on the surface of DNA coacervates by the addition of DOPC.[94] Copyright © 2022, The Author(s). (c) Formation of a phospholipid envelope on the surface of DNA coacervates by the addition of DPPC.[40] Copyright © 2021, American Chemical Society. (d) Lipid-coated coacervates exhibit reversible hypo-osmotic swelling and hyper-osmotic contraction during changes in the surrounding osmotic pressure.[95] Copyright © 2023, American Chemical Society. (e) Use of erythrocyte membrane fragments to encapsulate DNA coacervates.[97] Copyright © 2020, The Author(s), under exclusive license to Springer Nature Limited.

4 Biological Applications of DNA Coacervates

The unique advantages of DNA coacervates including biocompatibility, programmability, and sequestration ability make DNA coacervates highly promising candidates in the fields of biosensing and disease therapy. In this section, we summarize the significant progress in biological applications of DNA coacervates.

4.1. Biosensing applications of DNA coacervates

In recent years, DNA coacervates have been widely applied in the field of biosensing. The inherent high sequestration ability of DNA coacervates allows them to spontaneously capture small molecular analytes, and their compartmentalized nature facilitates signal amplification, thereby enhancing detection sensitivity. [100] Furthermore, DNA coacervates are typically synthesized using bottom-up approaches and exhibit programmability, enabling customization for specific analytes, which broadens their range of applications.

4.1.1. DNA coacervates for sensitive single-target detection

DNA coacervates have recently emerged as effective tools for detecting tumor-related markers. Li et al. demonstrated that DNA coacervates can significantly enhance the peroxidase-like activity of Hemin.[101] Loading the DNA G-quadruplex aptamer/Hemin complex (DGAH) formed from the binding of Hemin with DNA G-quadruplex aptamer into the liquid core of DNA coacervates can further increase their peroxidase-like activity. Based on these findings, their team developed an ultrasensitive method for detecting tumor-associated miRNA-25, a biomarker often linked to cancer progression. As illustrated in Figure 10a, they loaded DGAH into the liquid core of DNA coacervates through sequence design while anchoring molecular recognition elements on the surface of the DNA coacervates that specifically recognize target miRNA. Given that DNA coacervates enhanced the enzymatic activity of Hemin and improved the loading capacity of DGAH, which collectively improved the detection capability when the coacervates recognized the target, the 3,3′,5,5′-tetramethylbenzidine (TMB) in the solution would undergo a rapid chromogenic reaction, resulting in a color change from colorless to deep blue. The method they presented in this study achieves a detection limit (LOD) of 10 pM. Sun et al. proposed a DNA coacervates-based detection strategy that utilizes the hybridization chain reaction (HCR) to detect low-abundance intracellular miRNA.[102] As shown in Figure 10b, the authors encapsulated the mitochondrial-targeting (4-carboxybutyl) triphenylphosphonium bromide (TPP)-modified HP1 and the fluorescent probe-modified HP2 within tumor cell membrane vesicles to facilitate specific entry into target cells. Within the target cells, TPP-H1 specifically recognizes and binds to the miRNA target, inducing hybridization between TPP-HP1 and TAMRA-HP2, thereby initiating HCR to produce a large number of G-quadruplex precursors. Under the induction of K^+ within the cells, these precursors generate DNA coacervates based on G-quadruplex structures. Since G-quadruplex structures incorporate Hemin, they exhibit peroxidase-like activity, allowing them to convert TMB to TMB^+ in the presence of H_2O_2. This enables the detection of miRNA

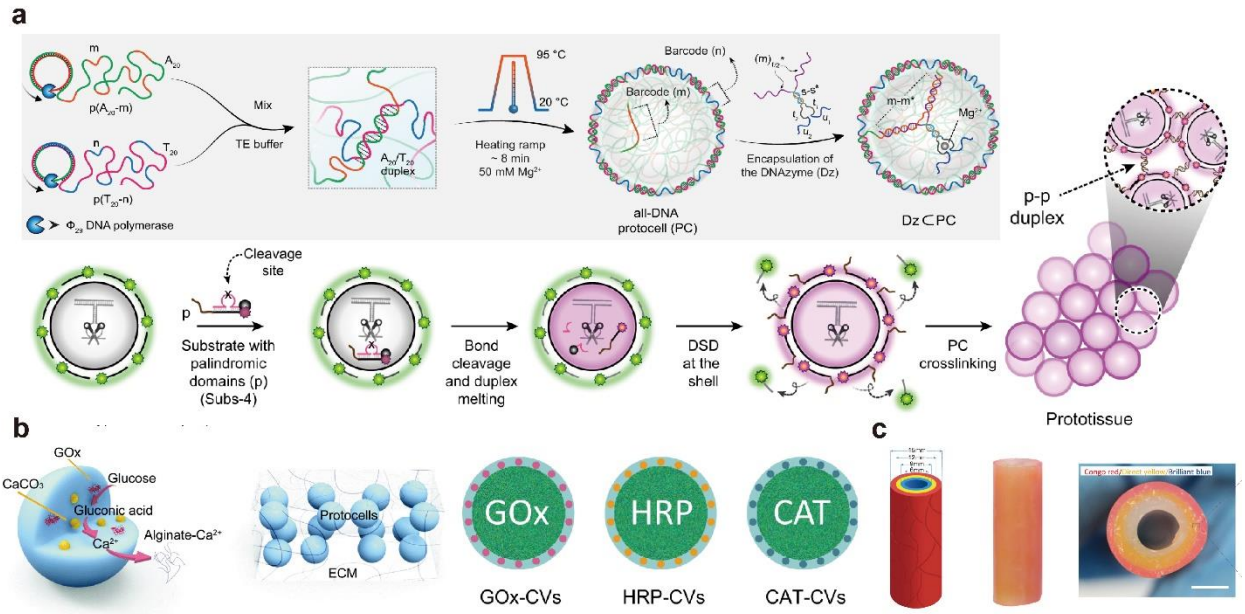

Figure 9 DNA coacervates used to mimic proto-tissue structures. (a) Driving the formation of tissue-like structures through the hybridization of ssDNA on the surface of DNA coacervate shells.[98] Copyright © 2022, The Author(s). (b) DNA coacervates catalysis Ca^{2+} production, which triggers tissue formation in natural calcium alginate hydrogels.[99] Copyright © 2021, Royal Society of Chemistry. (c) Formation of a hierarchical tissue vascular model using three different DNA coacervates.[94] Copyright © 2022, The Author(s)

concentrations by measuring absorbance at 652 nm. The study demonstrated a strong linear correlation between absorbance and the logarithm of miRNA-21 concentrations ranging from 10 pM to 10 μM, with a LOD of 1.10 pM.

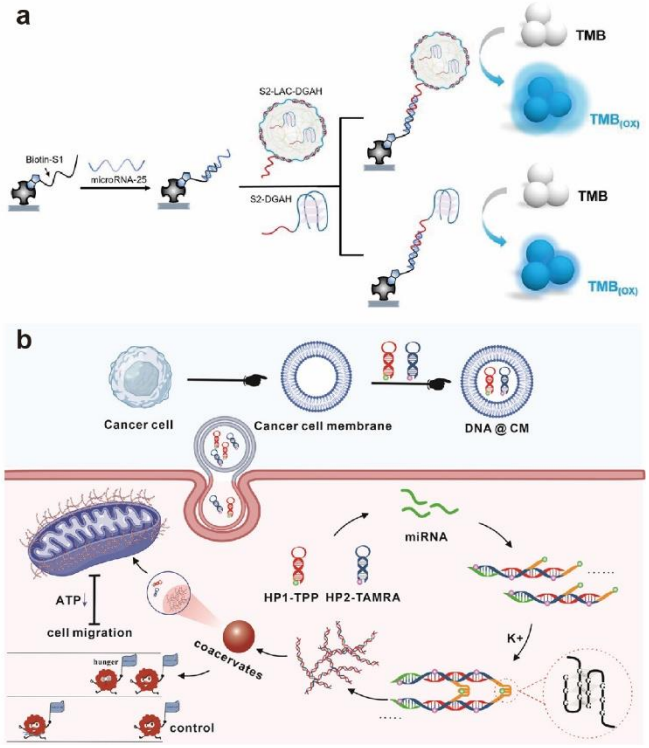

Figure 10 DNA coacervates used to detect biomarkers. (a) Schematic illustration of the mechanism of the designed sensing system based on DNA coacervates-DGAH or DGAH.[101] Copyright © 2023 Wiley-VCH GmbH. (b) Illustration of endogenous miRNA and K^+ co-activated dynamic assembly of DNA coacervates for intracellular miRNA imaging.[102] Copyright © 2023 American Chemical Society.

4.1.2. DNA coacervates for smart multi-parameter detection

For the diagnosis of diseases with complex molecular mechanisms, such as cancer, it is difficult to achieve sufficient specificity and sensitivity by detecting only a single target.[103] The introduction of logical operations has significantly enhanced the information processing capabilities of DNA coacervates, enabling multi-parameter detection of various biomarkers simultaneously and laying the foundation for clinical applications of DNA coacervates-based biosensing. In 2022, Liu et al. initiated efforts to integrate logical operations into DNA coacervates-based biosensing, aiming to enhance their capability for multi-input detection.[94] They prepared PDDA/DNA coacervates via LLPS and encapsulated them within a phospholipid membrane to generate DOPC-enveloped coacervate vesicles (DOPC-CV). Then, they immobilized DOPC-CV modified with palmitic acid (PA), GOx, HRP, and CAT onto the outer, middle, and inner layers of tubular model blood vessels, respectively, creating a dual-input/single-output device that mimics native tissue blood vessels (Figure 11a). When both glucose and hydroxylamine were present as dual inputs, the cascade reaction between GOx and HRP catalyzed the conversion of glucose to nitric oxide (NO), triggering a reaction with the Griess reagent that turned the solution purple. The excess intermediate product H_2O_2 was catalyzed by CAT to produce O_2, preventing a chromogenic reaction with 2,2'-azino-bis (3-ethylbenzothiazoline-6-sulfonic acid) (ABTS) in the system. The output of the AND logic gate operation was determined through colorimetric measurements. They explored four different input combinations and found that the absence of any single input failed to generate output "1", consistent with the rules of logical operations (Figure 11a). In the same year, Do et al. demonstrated the applicability of DNA coacervates in DNA logic operations.[53] Numerous studies have shown that Y-shaped DNA motifs with sticky ends can self-assemble into coacervates.[49] Based on these studies, Do et al. introduced short ssDNA to the Y-shaped motifs, enabling the coacervates to spontaneously enrich specific DNA strands through complementary base pairing and facilitate strand displacement reactions (Figure 11b). Their results indicated that the reaction rate for strand displacement within the coacervates was several times faster than that in solution. Inspired by these findings, they applied this design to a DNA logic circuit containing two layers of OR gates, resulting in significantly accelerated computational speeds, with enhancements ranging from 12 to 22 times

depending on the input types. Combining DNA logic operations with DNA coacervates for miRNA detection is a promising direction. In this regard, multiple miRNA targets are processed by Boolean logic gate, thus enabling multiple information processing. The rapid enrichment ability and compartmentalized environment of DNA coacervates provide an isolated environment for information processing, which enhances the sensitivity and specificity of miRNA detection.

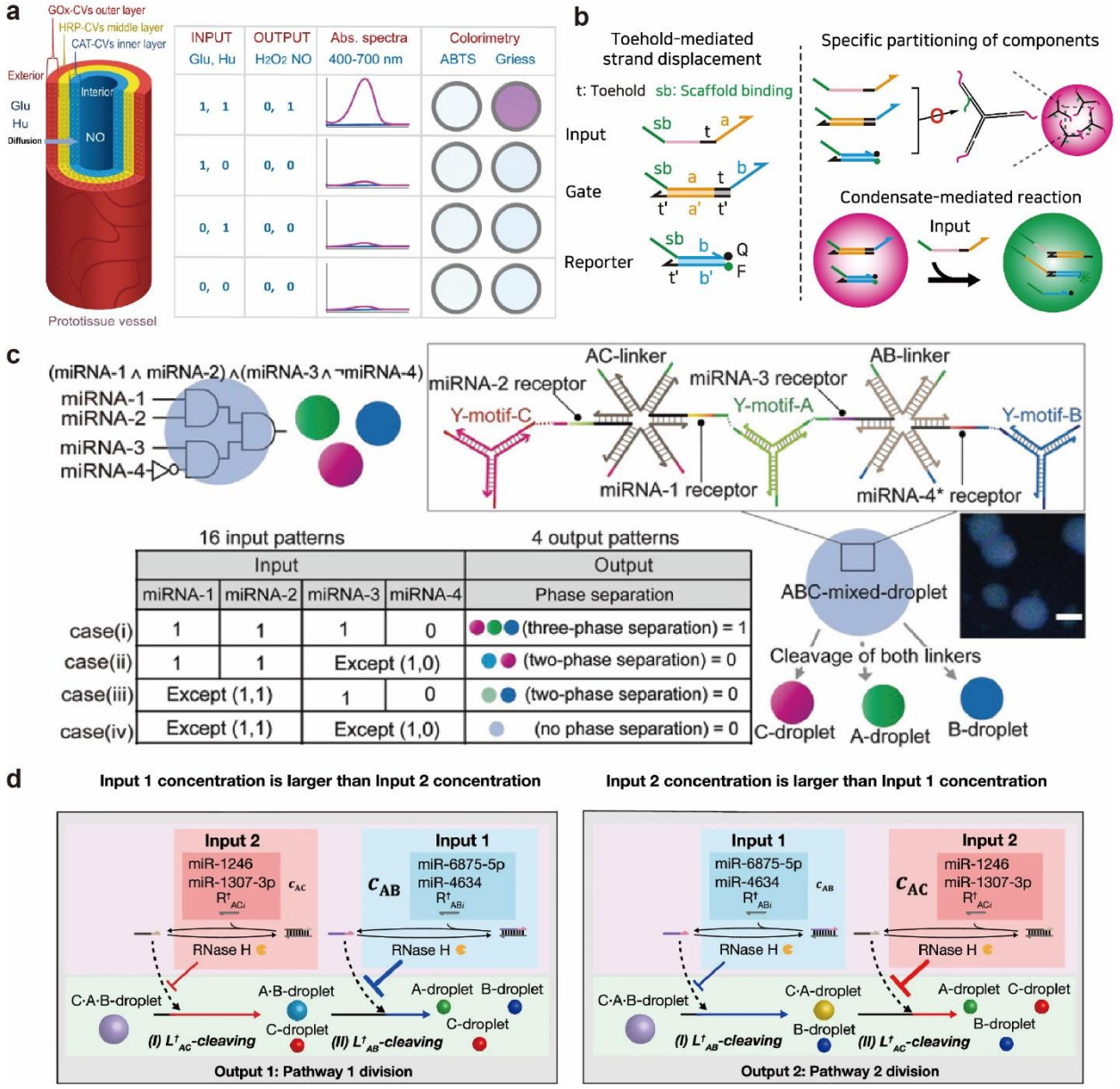

Figure 11 DNA coacervates used in logical operations. (a) Logic gate generation of NO in a three-layer tubular enzyme-CV modular proto-tissue like vessel demonstrating AND gate processing.[94] Copyright © 2022 Springer Nature. (b) Schematics of a double-cascade DNA strand displacement reaction and schematic of a two-layer OR gate and the truth table for different inputs.[53] Copyright © 2022 The Authors. (c) Computational DNA coacervates for four miRNA detections.[54] Copyright © 2022 The Authors. (d) Application of coacervates pathway control to a molecular comparator for miRNA concentrations.[84] Copyright © 2024 Springer Nature.

Gong et al. were also inspired by Y-shaped DNA motifs to develop a computational DNA coacervate with nucleic acid sensing capabilities, enabling the simultaneous detection of multiple miRNAs.[54] They designed three distinct Y-shaped DNA motif scaffolds to form DNA coacervates of types A, B, and C. Coacervates of the same type spontaneously fuse together due to DNA hybridization, while connections between different types require the linkers. When target miRNAs bind to the linkers, a strand displacement reaction occurs, leading to structural changes in the linkers and causing the division of the mixed coacervates into smaller DNA coacervates (Figure 11c). Different inputs result in varying outcomes of division among the mixed coacervates. The output can be "1" only when all four inputs are correct, indicating that three small coacervates are produced. Based on this principle, they constructed computational DNA coacervates that combine NOT and AND logic operations, successfully applying them to detect breast cancer biomarkers. The DNA coacervates based on Y-shaped DNA motifs can also serve as molecular computing elements for comparing the concentrations of different miRNAs. Tomoya et al. constructed three different coacervates using three types of Y-shaped DNA motifs. As previously described, these DNA coacervates require linkers for association, and the presence of trigger DNA initiates strand displacement reactions, ultimately resulting in the division of mixed coacervates.[84] To regulate the timing of this division, they introduced inhibitor strands and RNase H. The inhibitor strands can bind to the trigger DNA, preventing

strand displacement reactions, while RNase H can degrade the inhibitor strands, releasing the trigger DNA. By controlling the concentration of the inhibitor strands, they could manipulate the sequence of mixed coacervates division (Figure 11d). For example, when the concentration of inhibitor L†-AB exceeds that of L†-AC, the mixed coacervates preferentially divide to produce C before generating A and B. By designing the inhibitor chain as the miRNA to be tested, they were able to compare the concentrations of different miRNAs within the system. The authors utilized this approach to assess concentration differences among several breast cancer-associated miRNAs.

4.2. Therapeutic applications of DNA coacervates

4.2.1. DNA coacervate-based artificial immune system

One of the promising applications of DNA coacervates as a smart therapeutic platform is their ability to mimic the killing mechanisms of the cellular immune system. Specifically, DNA coacervates can be designed with DNA sequences to controllably capture or release functional modules in a simple manner, thereby inducing cell and bacterial death. Walczak et al. developed DNA coacervates to disrupt lipid membranes. These core-shell structured DNA coacervates consist of terminal cholesterol-modified DNA motifs as the core and two complementary DNA motifs as the outer shell.[64] When stimuli trigger the release of exterior DNA motifs, the exposed hydrophobic core causes the coacervates to attach to the GUV membrane. The accumulating of coacervates significantly destabilizes the GUV, typically leading to membrane rupture, which can be used for cell killing (Figure 12a). This behavior is analogous to the functions of the innate immune system, such as neutrophil extracellular traps, which release DNA networks in response to the stimulation by external signals, thereby capturing and killing pathogens.[104] To further mimic the activation-capture-kill process of neutrophils and the immune system, they also constructed a responsive drug release system. The branched portion of the DNA motif core was modified with i-motif sequences, that could induce the formation of the G-quadruplex structure after a decrease in pH resulting from natural glucose metabolism in E. coli. This process exposes hydrophobic core regions and forms a sticky DNA-cholesterol network for trapping and immobilizing bacteria to limit their movement. When giant unilamellar vesicles loaded with the antibiotic ciprofloxacin are added to the system, membrane rupture results in drug release. These drugs are released into bacteria immobilized by DNA coacervate traps to inhibit the growth and division of the captured bacteria (Figure 12b).[105] In a recent study, Li et al. developed a DNA-encoded artificial T cell mimetic model that is capable of accurately mimicking the kill behavior of T cells and inducing cancer cell death.[106] As illustrated in Figure 12c, the DNA coacervates respond to the acidic conditions of the tumor microenvironment and selectively release lipid-modified G-rich DNA strands. This process mimics the release of perforin upon the activation of cytotoxic T lymphocytes. Subsequently, the G-quadruplex structure efficiently integrates into the cell membranes of neighboring natural cells, serving as an artificial transmembrane channel for selective transport of K^+, which disrupts cellular homeostasis and ultimately induces apoptosis. Consequently, the utilization of DNA coacervates as intelligent immune cell mimics provides precise and controlled treatment to modulate cellular activity.

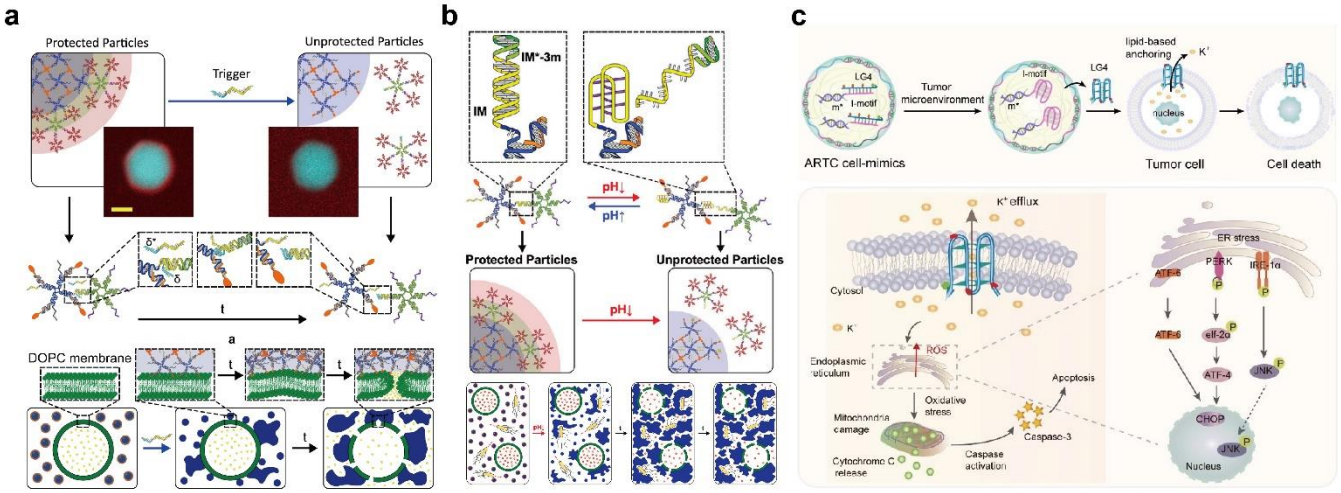

Figure 12 DNA coacervates mimicking the killing mechanism of the immune system. (a) Membrane disruption and permeabilization triggered by disassembly of cholesterol-bearing DNA coacervates.[64] Copyright © 2021, The Author(s). (b) Low pH-triggered bacterial capture and drug release.[105] Copyright © 2023 The Authors. Advanced Materials published by Wiley-VCH GmbH. (c) DNA-encoded artificial T-cell mimicry induces cellular apoptosis by releasing transmembrane channels in the mildly acidic microenvironment.[106] Copyright © 2024 Wiley-VCH GmbH.

4.2.2. DNA coacervate-based intelligent drug delivery system

Intelligent drug delivery systems improve drug targeting and efficacy while reducing side effects, making them essential for precise disease diagnosis and treatment. DNA coacervates can efficiently and conveniently concentrate therapeutically effective substances such as small molecules, biomolecules, and nanoparticles without the use of organic solvents. Due to the internal fluidity, material exchange can be easily achieved in DNA coacervates. This property allows them to function as drug slow-release systems within cells, realizing controlled release of drugs. Meanwhile, the good biocompatibility of DNA, unique aqueous environment and crowded molecules inside make coacervates favorable candidates to catalyze biochemical reactions and build programmable drug delivery platforms. As illustrated in Figure 13a, Hu et al. coated PEGylated phospholipids on the surface of DNA/PLL coacervates to prepare coacervates with membrane-like and cytoplasmic-like structures.[107] Uricase (Uri) and CAT are encapsulated within the DNA coacervates. This catalytic system not only efficiently degrades uric acid to allantoin and H_2O_2, but also converts the toxic intermediate H_2O_2 into O_2 and H_2O. The resulting O_2 can then continue to promote the catalytic degradation of uric acid, thereby enabling a persistent treatment of hyperuricemia. In addition, the PEGylated phospholipid coating can reduce the recognition of the reticuloendothelial system, thus prolonging systemic circulation time and protecting the activity of enzymes within the coacervate. Liu et al. constructed an invasion-defense interaction between DNA coacervates and living cells. The positively charged DNA coacervates containing GOx were internalized into host living cells through electrostatic interactions to establish the invasion process.[108] GOx promotes intracellular

glucose consumption and the generation of H_2O_2, which functions as reactive oxygen species (ROS) to inhibit cell proliferation. As a defense strategy, artificially introduced CAT is used to mediate intracellular H_2O_2 catabolism, scavenging ROS and protecting against ROS-induced cellular damage (Figure 13b). Besides using enzyme cascade reactions alone, Wang et al. constructed cascade-catalyzed coacervates loaded with GOx and copper peroxide nanodots (Cu NDs) to facilitate diabetic wound healing.[109] When applied to diabetic wounds, the DNA coacervate triggered the GOx-catalyzed oxidation of glucose in a hyperglycemic environment and the release of Cu^{2+} from decomposed Cu NDs in a localized acidic environment, both of which contributed to the catalyzed production of H_2O_2, acting as ROS to kill bacteria and promote wound healing (Figure 13c).

DNA coacervates can not only generate ROS through enzyme-catalyzed reactions, but also serve as reactors for NO production. Liu et al. successfully constructed synthetic cells with erythrocyte membrane structures by encapsulating GOx within DNA coacervates and wrapping phospholipid fragments of erythrocyte membranes around their surfaces.[97] Wrapping of erythrocyte membrane has been demonstrated to significantly improve the stability of the DNA coacervates and prolong their blood circulation time in vivo. When exposed to glucose and hydroxyurea, GOx within the coacervates utilized the glucose present in vivo to generate H_2O_2. H_2O_2 facilitated the conversion of hydroxyurea into NO signaling molecules, catalyzed by hemoglobin on the erythrocyte membrane, resulting in NO-mediated vasodilation. Additionally, synthetic proto-tissues with customized sizes, shapes, and spatial configurations can be designed as medical therapeutic models. Liu et al. constructed a hierarchical artificial blood vessel model using three DNA coacervates.[94] An enzymatic cascade reaction consisting of GOx, HRP, and CAT resulted in a sustained release of NO from the inner lumen of the artificial blood vessels. Meanwhile, residual potentially toxic H_2O_2 was efficiently scavenged, enhancing the NO-mediated anticoagulant activity. As mentioned above, the artificial vascular prototype exhibits a capacity for logical signal processing that depends on its spatial hierarchical structure, and a different order of bio-enzyme assembly would result in entirely distinct product outputs.

Due to the spontaneous coalescence inherent in LLPS, which is characterized by a high partition coefficient, DNA coacervates can serve as effective drug delivery platforms. These platforms enable the rapid recruitment and long-term retention of therapeutic agents, facilitating slow intracellular release and improving therapeutic efficacy. Ishak et al. employed chitosan-DNA coacervates to successfully achieve efficient delivery of the Jembrana DNA vaccine, improving its bioavailability and immunogenic response.[110] Zhou et al. encapsulated siRNA and proteins within PLL/ssDNA coacervates to successfully deliver the downregulated gene siBCL-2 and RNase A to cancer cells by using their efficient biomacromolecule loading, rapid cell internalization, and high cytosolic delivery efficiency, thus achieving a synergistic anti-tumor therapy.[111] However, DNA coacervates as drug delivery platforms still present challenges, such as spontaneous fusion properties and susceptibility to environmental factors, which lead to inhomogeneity and instability in drug delivery, thereby further limiting their application in vivo.[112] To address this issue, Liang et al. constructed an intracellular slow-release drug reservoir by in situ modulating LLPS to generate DNA coacervates within cells (Figure 13d).[113] First, histones were conjugated to DNA via a click reaction between trans-cyclooctene (TCO) and tetrazine (Tz) to form the 2E-conjugate, thereby preventing histones from participating in phase separation. Upon entering the cell, the 2E-conjugate gradually dissociates, releasing free histones and DNA, which restores their ability to undergo phase separation, ultimately resulting in the formation of an intracellular DNA coacervate drug reservoir. The drug reservoir is capable of actively enriching the small molecule drug doxorubicin (DOX) and increasing its size through the fusion of coacervates, thereby inhibiting drug excreting from multidrug-resistant tumor cells and prolonging its retention time. This approach maintained effective dosage and enhanced therapeutic efficacy, demonstrating significant effects against drug-resistant tumors in mouse models.

5. Conclusions and Perspectives

This paper tries to provide a comprehensive overview of the construction and application of DNA coacervates. We categorize different synthesis approaches of DNA coacervates and discuss the influencing factors. Then we summarize recent research progress on DNA coacervates, exploring their development as artificial cells in biomimetic applications and their role as a versatile platform in biosensing and therapeutics. Despite the booming research in this area, biomimetic and biological applications of DNA coacervates still face significant challenges.

First, the stability of DNA coacervates needs to be improved. The structural integrity of DNA coacervates is crucial for their proper function in complex biological environments. As previously mentioned, the coacervate state of DNA is influenced by factors such as ionic strength and pH. With increasing ionic concentration, DNA coacervates transition from a solid to a coacervate phase, and upon reaching the critical salt ion concentration, DNA coacervates revert to a homogeneous solution. However, the critical salt concentration for most coacervates is lower than physiological conditions. Additionally, due to the non-membrane nature of DNA coacervates, they are prone to self-fusion, wall adhesion, and easy disassembly, which instabilities significantly limit the application of DNA coacervates.[107] Another factor affecting the stability of DNA coacervates is their susceptibility to degradation by nucleases both inside and outside the cell, which further restricts their use in biological applications. To enhance the stability of DNA coacervates, strategies such as adding a phospholipid membrane on the surface or developing coacervates stable under physiological salt conditions can be employed. Furthermore, other modifications aimed at improving nuclease resistance can also effectively increase the stability of DNA coacervates. [114-116]

Secondly, the immunogenicity and specificity of DNA coacervates require further optimization. Although DNA itself is generally considered non-toxic to biological systems, the use of certain cationic reagents during the forming of these coacervates may trigger immune responses or pose toxicity concerns. Additionally, there is a need to incorporate specific targeting ligands and intelligent response mechanisms to improve the precision and effectiveness of drug delivery. Thirdly, optimizing the structural design is necessary to enhance the efficiency of large-scale production of DNA coacervates. The polymerization behavior of DNA molecules can be influenced by environmental factors, such as temperature, pH, and salt concentration,[32,55] potentially leading to inconsistencies or instability in the resulting structures. Therefore, it is vital to optimize environmental conditions and introduce novel self-assembly strategies that enhance the controllability and consistency of the self-assembly process. Additionally, microfluidic technology can be used to facilitate the rapid, efficient, and uniform generation of coacervates, thereby increasing overall yield. Typically, synthesizing DNA coacervates requires DNA concentrations at the mg/ml level, which can lead to significant costs. To address these challenges, researchers began using salmon sperm DNA as a raw material for synthesis.[97] However, the random sequence of salmon sperm DNA limits the construction of customizable-designed DNA coacervates. Therefore, there is a need to develop simpler and more cost-effective synthesis methods.

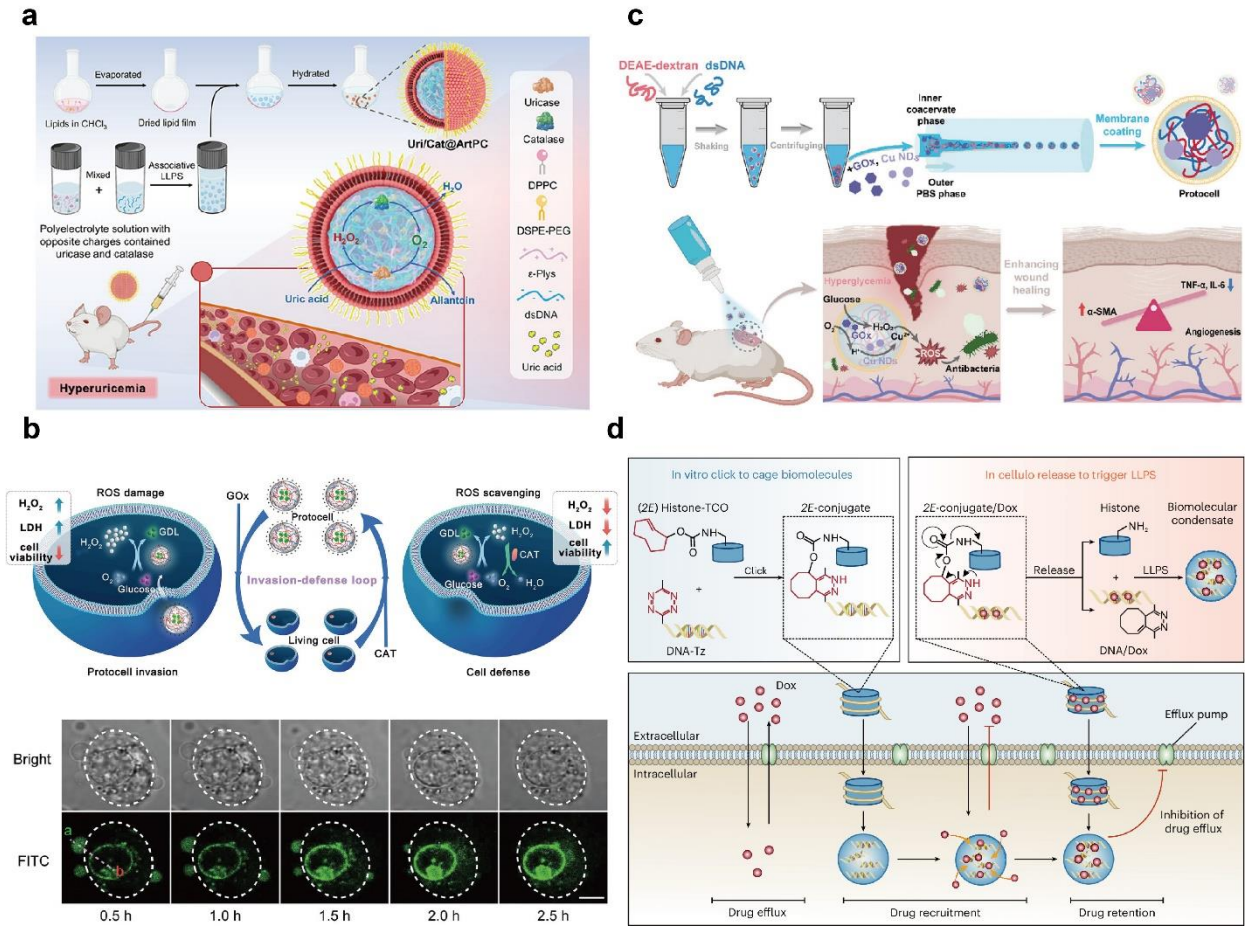

Figure 13 DNA coacervates are designed for drug delivery. (a) Schematic of the generation of Uri and CAT-loaded DNA coacervates and the working principle of treatment of hyperuricemia mice.[107] Copyright © 2023 Published by Elsevier B.V. (b) Schematic of the generation of GOx and Cu NDs-loaded DNA coacervates and the working principle of promoting diabetic wound healing.[109] Copyright © 2024 The Authors. Advanced Science published by Wiley-VCH GmbH. (c) Schematic of the invasion-defense mutual interaction between DNA coacervates and living cells.[108] Copyright © 2020 WILEY-VCH Verlag GmbH & Co. KGaA, Weinheim. (d) Schematic of the design of an LLPS-mediated intracellular drug reservoir and the working principle.[113] Copyright © 2024, The Author(s), under exclusive license to Springer Nature Limited.

Fourth, precise control of DNA coacervate phase separation remains a significant challenge. Due to the lack of membrane structures, DNA coacervates formed by charge interactions or DNA hybridization often fuse with one another at a specific condition, preventing the maintenance of independent compartmentalized structures. In the case of DNA coacervates formed by A-rich strands, since the strategy typically requires high-temperature annealing, it is not convenient to load temperature-sensitive cargos such as enzymes. Therefore, there is an urgent need to develop a more versatile controlling strategy or coacervate construction approach for the precise control of phase separation.

Fifth, achieving the programmability of DNA coacervate dynamics remains a significant challenge. Although some methods have been developed for dynamics regulation of DNA coacervates, they are highly sensitive to factors such as ionic strength and temperature. Furthermore, current methods are mainly limited for DNA coacervates formed through hybridization. For DNA coacervates formed through electrostatic interactions, however, their inherent instability makes them highly susceptible to environmental changes, which complicates the design of programmable systems. This issue becomes even more challenging when these coacervates are in complex biological environments. Therefore, eliminating external interference to achieve programmable dynamics while ensuring the structural and functional integrity of DNA coacervates requires further investigation.

Finally, current biomimetic applications of coacervates are largely limited to relatively simple enzyme cascade reactions. Besides, the range of stimulating factors and response signaling molecules developed to mimic intercellular communication remains restricted. These limitations pose a significant challenge in achieving more complex functions within DNA coacervates. Integrating functional biomolecules with DNA coacervates may be an effective solution. For example, Holtmannspötter et al. recently integrated DNAzymes with coacervates to upregulate or downregulate multiple reactions within a network, thereby mimicking the complexity of intracellular biological pathways.[117]

In conclusion, although DNA coacervates exhibit significant potential for biomimetic and biological applications, numerous challenges need to be addressed to enable their widespread use. The future development of this field may depend on several factors, including design optimization, advancements in synthesis technology, in-depth biomimetic research, and innovations in application areas, and will have a great impact on the fields of biomedicine, nanotechnology and materials science.[118]

Acknowledgement

This work was supported by the National Key Research and Development Project, China (No. 2020YFA0909000), the National Natural Science Foundation of China (No. 22107027), the Science and Technology Innovation Program of Hunan Province (No.

2024RC3099), the Natural Science Foundation of Hunan Province, China (No. 2023JJ20003), the Scientific Research Program of Furong Laboratory, China (No. 2023SK2088), and the Hunan Provincial Innovation Foundation for Postgraduate, China (No. CX20230409).

References

[1] Visser, B. S.; Lipiński, W. P.; Spruijt, E. The role of biomolecular condensates in protein aggregation. *Nat. Rev. Chem.* **2024,** *8*, 686-700.

[2] Pederson, T. The nucleolus. *Cold Spring Harb. Perspect. Biol.* **2011,** *3*, a000638.

[3] Gall, J. G. The centennial of the Cajal body. *Nat. Rev. Mol. Cell Biol.* **2003,** *4*, 975-980.

[4] Shin, Y.; Brangwynne, C. P. Liquid phase condensation in cell physiology and disease. *Science.* **2017,** *357*, eaaf4382.

[5] Miller, S. L.; Schopf, J. W.; Lazcano, A. Oparin's ``Origin of Life'': Sixty Years Later. *J. Mol. Evol.* **1997,** *44*, 351-353.

[6] Yu, X. L.; Zhou, L.; Wang, G. Y.; Wang, L.; Dou, H. J. Hierarchical Structures in Macromolecule-Assembled Synthetic Cells. *Macromol. Rapid Commun.* **2022,** *43*, 2100926.

[7] Seeman, N. C. DNA in a material world. *Nature.* **2003,** *421*, 427-431.

[8] Udono, H.; Gong, J.; Sato, Y.; Takinoue, M. DNA Droplets: Intelligent, Dynamic Fluid. *Advanced Biology.* **2023,** *7*, 2200180.

[9] Priftis, D.; Laugel, N.; Tirrell, M. Thermodynamic Characterization of Polypeptide Complex Coacervation. *Langmuir.* **2012,** *28*, 15947-15957.

[10] Vieregg, J. R.; Tang, T. D. Polynucleotides in cellular mimics: coacervates and lipid vesicles. *Curr. Opin. Colloid Interface Sci.* **2016,** *26*, 50-57.

[11] Bungenberg de Jong, H.; Kruyt, H. Proc. K. Ned. Akad. Wet, 1929; p 849-856.

[12] Teif, V. B.; Bohinc, K. Condensed DNA: condensing the concepts. *Prog. Biophys. Mol. Biol.* **2011,** *105*, 208-222.

[13] Razin, S.; Gavrilov, A. The role of liquid–liquid phase separation in the compartmentalization of cell nucleus and spatial genome organization. *Biochemistry (Moscow).* **2020,** *85*, 643-650.

[14] Alberti, S.; Gladfelter, A.; Mittag, T. Considerations and challenges in studying liquid-liquid phase separation and biomolecular condensates. *Cell.* **2019,** *176*, 419-434.

[15] Martin, N.; Tian, L. F.; Spencer, D.; Coutable-Pennarun, A.; Anderson, J. L. R.; Mann, S. Photoswitchable Phase Separation and Oligonucleotide Trafficking in DNA Coacervate Microdroplets. *Angew. Chem. Int. Ed.* **2019,** *58*, 14594-14598.

[16] Lu, T. M.; Spruijt, E. Multiphase Complex Coacervate Droplets. *J. Am. Chem. Soc.* **2020,** *142*, 2905-2914.

[17] Mountain, G. A.; Keating, C. D. Formation of Multiphase Complex Coacervates and Partitioning of Biomolecules within them. *Biomacromolecules.* **2020,** *21*, 630-640.

[18] Nakatani, N.; Sakuta, H.; Hayashi, M.; Tanaka, S.; Takiguchi, K.; Tsumoto, K.; Yoshikawa, K. Specific Spatial Localization of Actin and DNA in a Water/Water Microdroplet: Self-Emergence of a Cell-Like Structure. *Chembiochem.* **2018,** *19*, 1370-1374.

[19] Liu, X. J.; Xiong, Y. S.; Zhang, C. J.; Lai, R. J.; Liu, H.; Peng, R. Z.; Fu, T.; Liu, Q. L.; Fang, X. H.; Mann, S.et al. G-Quadruplex-Induced Liquid–Liquid Phase Separation in Biomimetic Protocells. *J. Am. Chem. Soc.* **2021,** *143*, 11036-11043.

[20] Nott, T. J.; Petsalaki, E.; Farber, P.; Jervis, D.; Fussner, E.; Plochowietz, A.; Craggs, T. D.; Bazett-Jones, D. P.; Pawson, T.; Forman-Kay, J. D. Phase transition of a disordered nuage protein generates environmentally responsive membraneless organelles. *Mol. Cell.* **2015,** *57*, 936-947.

[21] Ji, Y. L. M.; Li, F.; Qiao, Y. Modulating liquid–liquid phase separation of FUS: mechanisms and strategies. *J. Mater. Chem. B.* **2022,** *10*, 8616-8628.

[22] Koga, S.; Williams, D. S.; Perriman, A. W.; Mann, S. Peptide–nucleotide microdroplets as a step towards a membrane-free protocell model. *Nat. Chem.* **2011,** *3*, 720-724.

[23] Song, S. Y.; Ivanov, T.; Yuan, D. D.; Wang, J. Q.; da Silva, L. C.; Xie, J.; Cao, S. P. Peptide-Based Biomimetic Condensates via Liquid–Liquid Phase Separation as Biomedical Delivery Vehicles. *Biomacromolecules.* **2024,** *25*, 5468-5488.

[24] Jing, H. R.; Bai, Q. W.; Lin, Y. N.; Chang, H. J.; Yin, D. X.; Liang, D. H. Fission and Internal Fusion of Protocell with Membraneless "Organelles" Formed by Liquid–Liquid Phase Separation. *Langmuir.* **2020,** *36*, 8017-8026.

[25] Yin, Y. D.; Niu, L.; Zhu, X. C.; Zhao, M. P.; Zhang, Z. X.; Mann, S.; Liang, D. H. Non-equilibrium behaviour in coacervate-based protocells under electric-field-induced excitation. *Nat. Commun.* **2016,** *7*, 10658.

[26] Shapiro, J. T.; Leng, M.; Felsenfeld, G. Deoxyribonucleic acid-polylysine complexes. Structure and nucleotide specificity. *Biochemistry.* **1969,** *8*, 3219-3232.

[27] Vieregg, J.; Lueckheide, M.; Leon, L.; Marciel, A.; Tirrell, M. Nucleic acid-peptide complexes controlled by DNA hybridization. *Biophys. J.* **2016,** *110*, 566a.

[28] Wee, W. A.; Sugiyama, H.; Park, S. Photoswitchable single-stranded DNA-peptide coacervate formation as a dynamic system for reaction control. *IScience.* **2021,** *24*.

[29] Feric, M.; Vaidya, N.; Harmon, T. S.; Mitrea, D. M.; Zhu, L.; Richardson, T. M.; Kriwacki, R. W.; Pappu, R. V.; Brangwynne, C. P. Coexisting liquid phases underlie nucleolar subcompartments. *Cell.* **2016,** *165*, 1686-1697.

[30] Fraccia, T. P.; Martin, N. Non-enzymatic oligonucleotide ligation in coacervate protocells sustains compartment-content coupling. *Nat. Commun.* **2023,** *14*, 2606.

[31] Mao, S.; Kuldinow, D.; Haataja, M. P.; Košmrlj, A. Phase behavior and morphology of multicomponent liquid mixtures. *Soft Matter.* **2019,** *15*, 1297-1311.

[32] Vieregg, J. R.; Lueckheide, M.; Marciel, A. B.; Leon, L.; Bologna, A. J.; Rivera, J. R.; Tirrell, M. V. Oligonucleotide–Peptide Complexes: Phase Control by Hybridization. *J. Am. Chem. Soc.* **2018,** *140*, 1632-1638.

[33] Hayashi, K.; Chaya, H.; Fukushima, S.; Watanabe, S.; Takemoto, H.; Osada, K.; Nishiyama, N.; Miyata, K.; Kataoka, K. Influence of RNA strand rigidity on polyion complex formation with block catiomers. *Macromol. Rapid Commun.* **2016,** *37*, 486-493.

[34] Jing, H. R.; Chang, H. J.; Lin, Y. N.; Bai, Q. W.; Liang, D. H. Protocells with hierarchical structures as regulated by liquid–liquid and liquid–solid phase separations. *Chem. Commun.* **2020,** *56*, 12041-12044.

[35] Wang, Q. F.; Schlenoff, J. B. The Polyelectrolyte Complex/Coacervate Continuum. *Macromolecules.* **2014,** *47*, 3108-3116.

[36] Shakya, A.; King, J. T. DNA local-flexibility-dependent assembly of phase-separated liquid droplets. *Biophys. J.* **2018,** *115*, 1840-1847.

[37] Fraccia, T. P.; Jia, T. Z. Liquid Crystal Coacervates Composed of Short Double-Stranded DNA and Cationic Peptides. *ACS Nano.* **2020,** *14*, 15071-15082.

[38] Jia, T. Z.; Fraccia, T. P. Liquid Crystal Peptide/DNA Coacervates in the Context of Prebiotic Molecular Evolution. *Crystals.* **2020,** *10*, 964.

[39] Liu, Z. J.; Chen, J. X.; Bai, Q. W.; Lin, Y. N.; Liang, D. H. Coacervate

Formed by an ATP-Binding Aptamer and Its Dynamic Behavior under Nonequilibrium Conditions. *Langmuir.* **2022,** *38*, 6425-6434.

[40] Zhang, Y. W.; Chen, Y. F.; Yang, X. H.; He, X. X.; Li, M.; Liu, S. Y.; Wang, K. M.; Liu, J. B.; Mann, S. Giant Coacervate Vesicles As an Integrated Approach to Cytomimetic Modeling. *J. Am. Chem. Soc.* **2021,** *143*, 2866-2874.

[41] Chen, Y. F.; Yuan, M.; Zhang, Y. W.; Liu, S. Y.; Yang, X. H.; Wang, K. M.; Liu, J. B. Construction of coacervate-in-coacervate multi-compartment protocells for spatial organization of enzymatic reactions. *Chemical Science.* **2020,** *11*, 8617-8625.

[42] Peng, Y. H.; Hsiao, S. K.; Gupta, K.; Ruland, A.; Auernhammer, G. K.; Maitz, M. F.; Boye, S.; Lattner, J.; Gerri, C.; Honigmann, A.et al. Dynamic matrices with DNA-encoded viscoelasticity for cell and organoid culture. *Nat. Nanotechnol.* **2023,** *18*, 1463-1473.

[43] Merindol, R.; Delechiave, G.; Heinen, L.; Catalani, L. H.; Walther, A. Modular Design of Programmable Mechanofluorescent DNA Hydrogels. *Nat. Commun.* **2019,** *10*, 528.

[44] Benson, E.; Mohammed, A.; Gardell, J.; Masich, S.; Czeizler, E.; Orponen, P.; Högberg, B. DNA rendering of polyhedral meshes at the nanoscale. *Nature.* **2015,** *523*, 441-444.

[45] He, Y.; Ye, T.; Su, M.; Zhang, C.; Ribbe, A. E.; Jiang, W.; Mao, C. Hierarchical self-assembly of DNA into symmetric supramolecular polyhedra. *Nature.* **2008,** *452*, 198-201.

[46] Rossi-Gendron, C.; El Fakih, F.; Bourdon, L.; Nakazawa, K.; Finkel, J.; Triomphe, N.; Chocron, L.; Endo, M.; Sugiyama, H.; Bellot, G.et al. Isothermal self-assembly of multicomponent and evolutive DNA nanostructures. *Nat. Nanotechnol.* **2023,** *18*, 1311-1318.

[47] Li, L.; Yin, J.; Ma, W.; Tang, L. G.; Zou, J. H.; Yang, L. Z.; Du, T.; Zhao, Y.; Wang, L. H.; Yang, Z.et al. A DNA origami device spatially controls CD95 signalling to induce immune tolerance in rheumatoid arthritis. *Nat. Mater.* **2024,** *23*, 993-1001.

[48] Yin, J.; Wang, S. Y.; Wang, J. H.; Zhang, Y. W.; Fan, C. H.; Chao, J.; Gao, Y.; Wang, L. H. An intelligent DNA nanodevice for precision thrombolysis. *Nat. Mater.* **2024,** *23*, 854-862.

[49] Biffi, S.; Cerbino, R.; Bomboi, F.; Paraboschi, E. M.; Asselta, R.; Sciortino, F.; Bellini, T. Phase behavior and critical activated dynamics of limited-valence DNA nanostars. *Proc Natl Acad Sci.* **2013,** *110*, 15633-15637.

[50] Nguyen, D. T.; Jeon, B. J.; Abraham, G. R.; Saleh, O. A. Length-Dependence and Spatial Structure of DNA Partitioning into a DNA Liquid. *Langmuir.* **2019,** *35*, 14849-14854.

[51] Lee, T.; Do, S.; Lee, J. G.; Kim, D. N.; Shin, Y. The flexibility-based modulation of DNA nanostar phase separation. *Nanoscale.* **2021,** *13*, 17638-17647.

[52] Jeon, B. J.; Nguyen, D. T.; Saleh, O. A. Sequence-Controlled Adhesion and Microemulsification in a Two-Phase System of DNA Liquid Droplets. *The Journal of Physical Chemistry B.* **2020,** *124*, 8888-8895.

[53] Do, S.; Lee, C.; Lee, T.; Kim, D. N.; Shin, Y. Engineering DNA-based synthetic condensates with programmable material properties, compositions, and functionalities. *Sci.Adv.* **2022,** *8*, eabj1771.

[54] Gong, J.; Tsumura, N.; Sato, Y.; Takinoue, M. Computational DNA Droplets Recognizing miRNA Sequence Inputs Based on Liquid–Liquid Phase Separation. *Advanced Functional Materials.* **2022,** *32*, 2202322.

[55] Sato, Y.; Sakamoto, T.; Takinoue, M. Sequence-based engineering of dynamic functions of micrometer-sized DNA droplets. *Sci.Adv.* **2020,** *6*, eaba3471.

[56] Tran, M. P.; Chatterjee, R.; Dreher, Y.; Fichtler, J.; Jahnke, K.; Hilbert, L.; Zaburdaev, V.; Göpfrich, K. A DNA Segregation Module for Synthetic Cells. *Small.* **2023,** *19*, 2202711.

[57] Conrad, N.; Kennedy, T.; Fygenson, D. K.; Saleh, O. A. Increasing valence pushes DNA nanostar networks to the isostatic point. *Proc Natl Acad Sci.* **2019,** *116*, 7238-7243.

[58] Agarwal, S.; Dizani, M.; Osmanovic, D.; Franco, E. Light-controlled growth of DNA organelles in synthetic cells. *Interface Focus.* **2023,** *13*, 20230017.

[59] Nguyen, D. T.; Saleh, O. A. Tuning phase and aging of DNA hydrogels through molecular design. *Soft Matter.* **2017,** *13*, 5421-5427.

[60] Jeon, B. J.; Nguyen, D. T.; Abraham, G. R.; Conrad, N.; Fygenson, D. K.; Saleh, O. A. Salt-dependent properties of a coacervate-like, self-assembled DNA liquid. *Soft Matter.* **2018,** *14*, 7009-7015.

[61] Agarwal, S.; Osmanovic, D.; Klocke, M. A.; Franco, E. The Growth Rate of DNA Condensate Droplets Increases with the Size of Participating Subunits. *ACS Nano.* **2022,** *16*, 11842-11851.

[62] Sato, Y.; Takinoue, M. Sequence-dependent fusion dynamics and physical properties of DNA droplets. *Nanoscale Advances.* **2023,** *5*, 1919-1925.

[63] Leathers, A.; Walczak, M.; Brady, R. A.; Al Samad, A.; Kotar, J.; Booth, M. J.; Cicuta, P.; Di Michele, L. Reaction–Diffusion Patterning of DNA-Based Artificial Cells. *J. Am. Chem. Soc.* **2022,** *144*, 17468-17476.

[64] Walczak, M.; Brady, R. A.; Mancini, L.; Contini, C.; Rubio-Sánchez, R.; Kaufhold, W. T.; Cicuta, P.; Di Michele, L. Responsive core-shell DNA particles trigger lipid-membrane disruption and bacteria entrapment. *Nat. Commun.* **2021,** *12*, 4743.

[65] Deng, J.; Walther, A. Programmable ATP-fueled DNA coacervates by transient liquid-liquid phase separation. *Chem.* **2020,** *6*, 3329-3343.

[66] Liu, W.; Deng, J.; Song, S. Y.; Sethi, S.; Walther, A. A facile DNA coacervate platform for engineering wetting, engulfment, fusion and transient behavior. *Communications Chemistry.* **2024,** *7*, 100.

[67] Merindol, R.; Loescher, S.; Samanta, A.; Walther, A. Pathway-controlled formation of mesostructured all-DNA colloids and superstructures. *Nat. Nanotechnol.* **2018,** *13*, 730-738.

[68] Liu, W.; Samanta, A.; Deng, J.; Akintayo, C. O.; Walther, A. Mechanistic Insights into the Phase Separation Behavior and Pathway-Directed Information Exchange in all-DNA Droplets. *Angew. Chem. Int. Ed.* **2022,** *61*, e202208951.

[69] Ralec, C.; Henry, E.; Lemor, M.; Killelea, T.; Henneke, G. Calcium-driven DNA synthesis by a high-fidelity DNA polymerase. *Nucleic Acids Res.* **2017,** *45*, 12425-12440.

[70] Korolev, N.; Lyubartsev, A. P.; Rupprecht, A.; Nordenskiöld, L. Competitive binding of Mg2+, Ca2+, Na+, and K+ ions to DNA in oriented DNA fibers: experimental and Monte Carlo simulation results. *Biophys. J.* **1999,** *77*, 2736-2749.

[71] Ahmad, R.; Arakawa, H.; Tajmir-Riahi, H. A comparative study of DNA complexation with Mg (II) and Ca (II) in aqueous solution: major and minor grooves bindings. *Biophys. J.* **2003,** *84*, 2460-2466.

[72] Kumar, B. V. V. S. P.; Patil, A. J.; Mann, S. Enzyme-powered motility in buoyant organoclay/DNA protocells. *Nat. Chem.* **2018,** *10*, 1154-1163.

[73] Jang, W. S.; Kim, H. J.; Gao, C.; Lee, D.; Hammer, D. A. Enzymatically Powered Surface-Associated Self-Motile Protocells. *Small.* **2018,** *14*, 1801715.

[74] Qiao, Y.; Li, M.; Booth, R.; Mann, S. Predatory behaviour in synthetic protocell communities. *Nat. Chem.* **2017,** *9*, 110-119.

[75] Gao, N.; Xu, C.; Yin, Z. P.; Li, M.; Mann, S. Triggerable Protocell Capture in Nanoparticle-Caged Coacervate Microdroplets. *J. Am. Chem. Soc.* **2022,** *144*, 3855-3862.

[76] Mu, W.; Jia, L.; Zhou, M.; Wu, J.; Lin, Y.; Mann, S.; Qiao, Y. Superstructural ordering in self-sorting coacervate-based protocell networks. *Nat. Chem.* **2024,** *16*, 158-167.

[77] Qiao, Y.; Li, M.; Qiu, D.; Mann, S. Response-retaliation behavior in synthetic protocell communities. *Angew. Chem.* **2019,** *131*, 17922-

17927.

[78] Joesaar, A.; Yang, S.; Bögels, B.; van der Linden, A.; Pieters, P.; Kumar, B. V. V. S. P.; Dalchau, N.; Phillips, A.; Mann, S.; de Greef, T. F. A. DNA-based communication in populations of synthetic protocells. *Nat. Nanotechnol.* **2019,** *14*, 369-378.

[79] Ji, Y. l. M.; Lin, Y. Y.; Qiao, Y. Plant Cell-Inspired Membranization of Coacervate Protocells with a Structured Polysaccharide Layer. *J. Am. Chem. Soc.* **2023,** *145*, 12576-12585.

[80] Rothemund, P. W. K. Folding DNA to create nanoscale shapes and patterns. *Nature.* **2006,** *440*, 297-302.

[81] Koshland, D. E. The Seven Pillars of Life. *Science.* **2002,** *295*, 2215-2216.

[82] Wilken, S.; Chaderjian, A.; Saleh, O. A. Spatial Organization of Phase-Separated DNA Droplets. *Physical Review X.* **2023,** *13*, 031014.

[83] Samanta, A.; Sabatino, V.; Ward, T. R.; Walther, A. Functional and morphological adaptation in DNA protocells via signal processing prompted by artificial metalloenzymes. *Nat. Nanotechnol.* **2020,** *15*, 914-921.

[84] Maruyama, T.; Gong, J.; Takinoue, M. Temporally controlled multistep division of DNA droplets for dynamic artificial cells. *Nat. Commun.* **2024,** *15*, 7397.

[85] Saleh, O. A.; Jeon, B. J.; Liedl, T. Enzymatic degradation of liquid droplets of DNA is modulated near the phase boundary. *Proc Natl Acad Sci.* **2020,** *117*, 16160-16166.

[86] Saleh, O. A.; Wilken, S.; Squires, T. M.; Liedl, T. Vacuole dynamics and popping-based motility in liquid droplets of DNA. *Nat. Commun.* **2023,** *14*, 3574.

[87] Deng, N. N.; Huck, W. T. S. Microfluidic Formation of Monodisperse Coacervate Organelles in Liposomes. *Angew. Chem. Int. Ed.* **2017,** *56*, 9736-9740.

[88] Malouf, L.; Tanase, D. A.; Fabrini, G.; Brady, R. A.; Paez-Perez, M.; Leathers, A.; Booth, M. J.; Di Michele, L. Sculpting DNA-based synthetic cells through phase separation and phase-targeted activity. *Chem.* **2023,** *9*, 3347-3364.

[89] Waters, C. M.; Bassler, B. L. QUORUM SENSING: Cell-to-Cell Communication in Bacteria. *Annu. Rev. Cell Dev. Biol.* **2005,** *21*, 319-346.

[90] Zhao, Q. H.; Cao, F. H.; Luo, Z. H.; Huck, W. T. S.; Deng, N.-N. Photoswitchable Molecular Communication between Programmable DNA-Based Artificial Membraneless Organelles. *Angew. Chem. Int. Ed.* **2022,** *61*, e202117500.

[91] Chen, H.; Xu, W. Y.; Shi, H.; Qiao, Y.; He, X. X.; Zheng, J.; Zhou, S. H.; Yang, X. H.; Wang, K. M.; Liu, J. B. DNA-Based Artificial Receptors as Transmembrane Signal Transduction Systems for Protocellular Communication. *Angew. Chem. Int. Ed.* **2023,** *62*, e202301559.

[92] Abbas, M.; Lipiński, W. P.; Wang, J.; Spruijt, E. Peptide-based coacervates as biomimetic protocells. *Chem. Soc. Rev.* **2021,** *50*, 3690-3705.

[93] Dora Tang, T. Y.; Rohaida Che Hak, C.; Thompson, A. J.; Kuimova, M. K.; Williams, D. S.; Perriman, A. W.; Mann, S. Fatty acid membrane assembly on coacervate microdroplets as a step towards a hybrid protocell model. *Nature Chemistry.* **2014,** *6*, 527-533.

[94] Liu, S. Y.; Zhang, Y. W.; He, X. X.; Li, M.; Huang, J.; Yang, X. H.; Wang, K. M.; Mann, S.; Liu, J. B. Signal processing and generation of bioactive nitric oxide in a model prototissue. *Nat. Commun.* **2022,** *13*, 5254.

[95] Zhang, Y. W.; Wang, Z. F.; Li, M.; Xu, C.; Gao, N.; Yin, Z. P.; Wang, K. M.; Mann, S.; Liu, J. B. Osmotic-Induced Reconfiguration and Activation in Membranized Coacervate-Based Protocells. *J. Am. Chem. Soc.* **2023,** *145*, 10396-10403.

[96] Chang, H. J.; Jing, H. R.; Yin, Y. D.; Zhang, Q. F; Liang, D. H. Membrane-mediated transport in a non-equilibrium hybrid protocell based on coacervate droplets and a surfactant. *Chem. Commun.* **2018,** *54*, 13849-13852.

[97] Liu, S. Y.; Zhang, Y. W.; Li, M.; Xiong, L.; Zhang, Z. J.; Yang, X. H.; He, X. X.; Wang, K. M.; Liu, J. B.; Mann, S. Enzyme-mediated nitric oxide production in vasoactive erythrocyte membrane-enclosed coacervate protocells. *Nat. Chem.* **2020,** *12*, 1165-1173.

[98] Samanta, A.; Hörner, M.; Liu, W.; Weber, W.; Walther, A. Signal-processing and adaptive prototissue formation in metabolic DNA protocells. *Nat. Commun.* **2022,** *13*, 3968.

[99] Chen, Y. F.; Zhang, Y. W.; Li, M.; Liu, S. Y.; Yang, X. H.; Wang, K. M.; Mann, S.; Liu, J. B. Self-immobilization of coacervate droplets by enzyme-mediated hydrogelation. *Chem. Commun.* **2021,** *57*, 5438-5441.

[100] Smokers, I. B.; Visser, B. S.; Slootbeek, A. D.; Huck, W. T.; Spruijt, E. How Droplets Can Accelerate Reactions— Coacervate Protocells as Catalytic Microcompartments. *Acc. Chem. Res.* **2024,** *57*, 1885-1895.

[101] Li, J. C.; Yang, C.; Zhang, L. Z.; Li, C. Y.; Xie, S. T.; Fu, T.; Zhang, Z. W.; Li, L. J.; Qi, L. B.; Lyu, Y. F.et al. Phase Separation of DNA-Encoded Artificial Cells Boosts Signal Amplification for Biosensing. *Angew. Chem. Int. Ed.* **2023,** *62*, e202306691.

[102] Sun, W.; Yin, J.; Liu, L.; Wu, Z.; Wang, Y.; Liu, T.; Xiong, H.; Liu, X.; Wang, X.; Jiang, H. Endogenous miRNA and K+ Co-Activated Dynamic Assembly of DNA Coacervates for Intracellular miRNA Imaging and Mitochondrial Intervention. *Anal. Chem.* **2023,** *95*, 14101-14110.

[103] Hu, R.; Wang, X. W.; Zhan, X. Q. Multi-parameter systematic strategies for predictive, preventive and personalised medicine in cancer. *EPMA Journal.* **2013,** *4*, 1-12.

[104] Brinkmann, V.; Reichard, U.; Goosmann, C.; Fauler, B.; Uhlemann, Y.; Weiss, D. S.; Weinrauch, Y.; Zychlinsky, A. Neutrophil Extracellular Traps Kill Bacteria. *Science.* **2004,** *303*, 1532-1535.

[105] Walczak, M.; Mancini, L.; Xu, J.; Raguseo, F.; Kotar, J.; Cicuta, P.; Di Michele, L. A Synthetic Signaling Network Imitating the Action of Immune Cells in Response to Bacterial Metabolism. *Adv. Mater.* **2023,** *35*, 2301562.

[106] Li, C. Y.; Wang, D.; Gao, H. Y.; Fu, T.; He, L.; Han, D.; Tan, W. H. Leveraging DNA-Encoded Cell-Mimics for Environment-Adaptive Transmembrane Channel Release-Induced Cell Death. *Angew. Chem. Int. Ed.* **2024,** *63*, e202406186.

[107] Hu, Q.; Lan, H. B.; Tian, Y. M.; Li, X. N.; Wang, M. M.; Zhang, J.; Yu, Y. L.; Chen, W.; Kong, L.; Guo, Y. Y. Biofunctional coacervate-based artificial protocells with membrane-like and cytoplasm-like structures for the treatment of persistent hyperuricemia. *J. Controlled Release.* **2024,** *365*, 176-192.

[108]Zhang, Y. W.; Liu, S. Y.; Yao, Y.; Chen, Y. F.; Zhou, S. H.; Yang, X. H.; Wang, K. M.; Liu, J. B. Invasion and Defense Interactions between Enzyme-Active Liquid Coacervate Protocells and Living Cells. *Small.* **2020,** *16*, 2002073.

[109] Wang, C.; Yang, X. Y.; Wang, Q.; Zhang, L. Y.; Shang, L. R. Glucose Responsive Coacervate Protocells from Microfluidics for Diabetic Wound Healing. *Advanced Science.* **2024,** *11*, 2400712.

[110] Ishak, J.; Unsunnidhal, L.; Martien, R.; Kusumawati, A. evaluation of chitosan-DNA plasmid complex encoding Jembrana disease virus env-tm protein as a vaccine candidate. *Journal of Veterinary Research.* **2019,** *63*, 7-16.

[111] Zhou, Q.; Xiang, J. J.; Hao, L. Q.; Xu, X. J.; Zhou, Z. X.; Tang, J. B.; Ping, Y.; Shen, Y. Q. Polyplex nanovesicles of single strand oligonucleotides for efficient cytosolic delivery of biomacromolecules. *Nano Today.* **2021,** *39*, 101221.

[112] Zhao, P. C.; Guo, J. X.; Jiang, T. S.; Xu, X. Y.; Chen, S. R.; Li, Z.; Xu, J. K.; Li, G.; Bian, L. m. Vacuolated coacervate mediates the bimodal release kinetics of diverse macromolecular drugs in vivo. *Materials Today.* **2023,** *66*, 26-35.

[113] Liang, T. X.; Dong, Y. X.; Cheng, L.; Wen, P.; Li, F. Q.; Liu, F.; Wu, Q.; Ren, E.; Liu, P. F.; Li, H. J.et al. In situ formation of biomolecular condensates as intracellular drug reservoirs for augmenting chemotherapy. *Nat. Biomed. Eng.* **2024**, 1-14.

[114] Thirunavukarasu, D.; Chen, T.; Liu, Z.; Hongdilokkul, N.; Romesberg, F. E. Selection of 2 ′ -Fluoro-Modified Aptamers with Optimized Properties. *J. Am. Chem. Soc.* **2017,** *139*, 2892-2895.

[115] Roberts, T. C.; Langer, R.; Wood, M. J. A. Advances in oligonucleotide drug delivery. *Nat. Rev. Drug Discovery.* **2020,** *19*, 673-694.

[116] Yang, B.; Zhou, B.; Li, C. F.; Li, X. W.; Shi, Z. W.; Li, Y. X.; Zhu, C. Y.; Li, X.; Hua, Y.; Pan, Y. F.et al. A Biostable l-DNA Hydrogel with Improved Stability for Biomedical Applications. *Angew. Chem. Int. Ed.* **2022,** *61*, e202202520.

[117] Holtmannspötter, A.-L.; Machatzke, C.; Begemann, C.; Salibi, E.; Donau, C.; Späth, F.; Boekhoven, J.; Mutschler, H. Regulating nucleic acid catalysis using active droplets. *Angew. Chem. Int. Ed.* **2024**, e202412534.

[118] Huang, Z. Y.; Wang, D.; Zhang, Q.; Zhang, Y. T.; Peng, R.; Tan, W. H. Leveraging Aptamer-Based DNA Nanotechnology for Bioanalysis and Cancer Therapeutics. *Accounts of Materials Research.* **2024,** *5*, 438-452.

Left to Right: Yuqi Zeng, Long Zhao, Yihao Liu, Tianhuan Peng*, Yifan Lyu*, Quan Yuan*.

Yuqi Zeng is currently a Ph.D. candidate at the College of Biology, Hunan University, under the supervision of Prof. Yifan Lyu and Prof. Weihong Tan. She received her B.E. degree in chemistry from Yunnan normal University in 2022. Her current research focuses on the design of dynamic DNA probes for bio-imaging and bioanalysis, and the construction of bionic artificial cells.

Long Zhao is currently a master's candidate at the College of Biology, Hunan University, under the supervision of Prof. Yifan Lyu and Prof. Weihong Tan. She received her B.E. degree in Biology from Hunan University in 2023. Her current research focuses on DNA logic circuits and the design of dynamic DNA probes for bio-imaging and bioanalysis.

Yihao Liu is currently a Ph.D. candidate at the College of Chemistry and Chemical Engineering, Hunan University, under the supervision of Prof. Yifan Lyu and Prof. Weihong Tan. He received his B.E. degree in chemistry from Hunan University in 2020. His current research focuses on the DNA dynamic nanotechnology and artificial cell.

Tianhuan Peng is an assistant professor in the College of Biology at Hunan University. He received his B.S. degree in 2012 from Beijing University of Chemical Technology and his Ph.D. degree in 2017 from the Shanghai Institute of Applied Physics, Chinese Academy of Sciences. He pursued postdoctoral research at Hunan University from 2017 to 2020. His research interests concentrate on the development and application of functional nucleic acid molecules.

Yifan Lyu is an associate professor of College of Chemistry and Chemical Engineering at Hunan University. He received his B.S. degree in 2012 and Ph.D. degree in 2017 from Hunan University. During his Ph. D education, he spent two years as a joint-visiting student at the University of Florida in the US. He pursued postdoctoral research at Shanghai Jiao Tong University from 2018 to 2020. His research interests focus on DNA nanotechnology and artificial cell.

Quan Yuan is a professor in Hunan University. She received her B.S. degree from Wuhan University in 2004 and Ph.D. degree in inorganic chemistry from Peking University in 2009. Afterwards, she worked as a postdoctoral researcher at the University of Florida from 2009 to 2011. Her research focuses on the bioassays of complex samples.

Entry for the Table of Contents

Biomimetic and biological applications of DNA coacervates

Yuqi Zeng,‡ Long Zhao,‡ Yihao Liu, Tianhuan Peng, * Yifan Lyu, * and Quan Yuan*

Chin. J. Chem. **2024**, *42*, XXX—XXX. **DOI: 10.1002/cjoc.202400XXX**

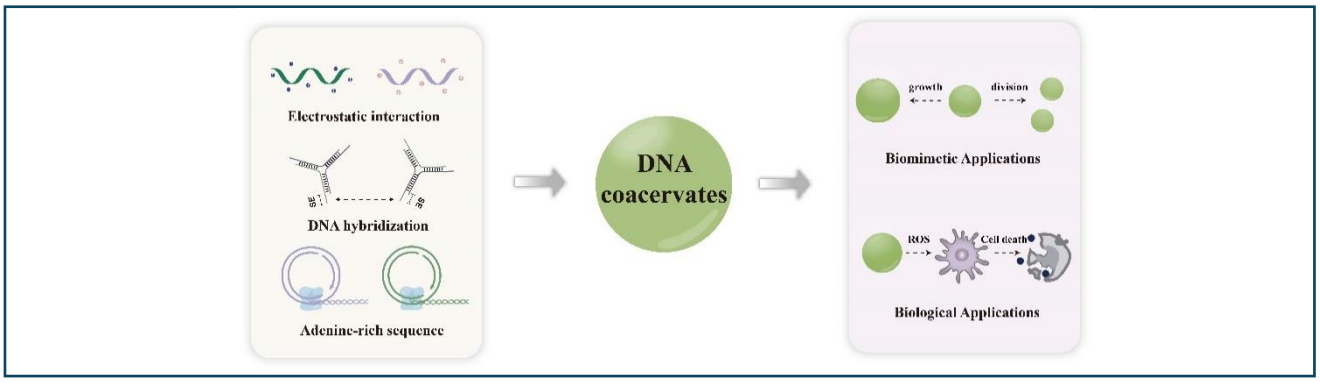

This review describes the formation mechanisms of different kinds of DNA coacervates, with a particular focus on their recent advances in mimicking cellular behaviors, cell communication, and tissue formation, as well as their potential applications in biosensing and biomedicine. Furthermore, the challenges faced by DNA-based coacervates in biomimetic and biological applications are discussed and future directions of this field are prospected.

